PERFORMANCE SENSORS FOR A RACING WHEELCHAIR

Lappeenranta–Lahti University of Technology LUT

Master's Program in Mechatronic System Design, Master's Thesis

2022

Achal Agasthya

Examiner(s): Professor Aki Mikkola

D.Sc. (Tech) Kimmo Kerkkänen

ABSTRACT

Lappeenranta–Lahti University of Technology LUT

LUT School of Energy Systems

Mechanical Engineering

Achal Agasthya

Performance sensors for a racing wheelchair

Master's thesis

2022

91 pages, 41 figures, 8 tables and 3 appendices

Examiners: Professor Aki Mikkola and D.Sc. (Tech) Kimmo Kerkkänen

Keywords: Wheelchair racing, Power meter, Finite Element Analysis, Systematic Machine Design, DFMA

Because of the relevance and popularity of paralympic wheelchairs, players and coaches have been focusing on a variety of performance enhancements. The athlete's performance or the equipment they utilize, in this case, a racing wheelchair, can be measured. Performance is often quantified using a variety of characteristics, with a concentration on power measurement.

The purpose of this thesis is to investigate the application of a Quarq Dzero Dub cycling power meter in a racing wheelchair. The power meter is a crankset power meter that measures a rider's torque input and converts it to power in Watts.

A thorough literature analysis reveals three approaches for measuring power in a wheelchair that were not used in this thesis. The power measuring idea employed in the study overcame its limits, which were not relevant to the research problem of this study. A comprehensive design procedure was conducted where all parts were designed according to the size and criteria of the power meter in a full design method using Solidworks 2020. This was followed by the model being evaluated under static stress and the strength-to-weight ratio was calculated using static analysis and topological analysis. The findings were then thoroughly examined to determine their validity and reliability.

Because of the alterations made to the push rim, which allows force transfer from the athlete to the power meter, the power meter can detect power at the hub of the wheel assembly, as shown in this report.

ACKNOWLEDGEMENTS

First and foremost, I want to express my gratitude to Professor Aki Mikkola and Kimmo Kerkkänen for believing in me and allowing me to pursue this research project. I will always be grateful for their unwavering encouragement, motivation, and patience. They are incredibly amazing to work with and continually encouraged me to explore and attempt alternative solutions to problems and were always there for me when I was struggling in situations where I needed their help.

This thesis would not have been possible without my parents' constant encouragement. They have always been extremely supportive of me in all my endeavours, and I would not be in this position without them. I'd also like to express my gratitude to my friends and family for their support, encouragement, and well-wishes for my success.

Thank you!

Achal Agasthya

Achal Agasthya

Lappeenranta 08.05.2022

SYMBOLS AND ABBREVIATIONS

Roman characters

A	Area	[m^2 or mm^2]
d	Diameter	[mm]
r_{dym}	Dynamic radius	[m]
F	Force	[N]
f	Frictional factor	
l	Length	[mm]
M_{bmax}	Maximum bending moment	[Nm]
M	Moment	[Nmm]
P	Power	[Watts]
F_r	Radial force	[N]
Z	Section modulus	[mm^3]
F_{static}	Static wheel load	[N]
ε	Strain	
F_t	Tangential force	[N]
t	Time	[s]
W	Work done	[J]

Greek characters

μ	coefficient of friction	
Π	pi	
τ	torque	[Nm]

Abbreviations

BCD	Bolt Circle Diameter
CAD	Computer Aided Design
DFMA	Design for Manufacturing and Assembly
FEA	Finite Element Analysis
GPU	Graphics Processing Unit
PO	Power Output
SMD	Systematic Machine Design
TDC	Top Dead Centre
2-D	Two Dimensional
3-D	Three Dimensional

Table of contents

Abstract

Acknowledgements

Symbols and Abbreviations

1. Introduction 3
   1.1. Background 3
   1.2. Project objectives and research questions 5
   1.3. Methodology 7
2. Literature Review of power measurement approaches 8
   2.1. Previous approaches in power measurement 8
      2.1.1. Strain Gauges 8
      2.1.2. Tactile Gloves 13
      2.1.3. Custom Wheelchair Push Rim 16
   2.2. Power measurement in wheelchairs 21
   2.3. Paralympic Wheelchair Dynamics 26
      2.3.1. Dynamics of wheelchair 26
      2.3.2. Forces on a wheelchair 29
   2.4. Design and analysis of wheelchair power meter 32
   2.5. DFMA Analysis 35
3. CAD design and assembly of wheelchair-power meter 37
   3.1. Design Scope and Boundaries 39
   3.2. Design Process 40
      3.2.1. Design Problem 40
      3.2.2. Brainstorming 41
      3.2.3. Design Plan and Creation 41
      3.2.4. Testing and Improvement 42
   3.3. CAD Modelling 43
4. Results and Discussion 50
   4.1. FEA analysis 50

4.2. Discussion 58
5. Conclusions 60
References 63

Appendices

Appendix 1. Tables containing comparisons between different power meters

Appendix 2. Systematic Machine Design Concepts

Appendix 3. Alternate 3-D design and analysis of wheelchair-power meter assembly

1. Introduction

Performance analysis determines how well an instrument, vehicle, person, or other entity performs in each task. When anything is immobile or in motion, performance can be measured. The study of an object in motion is termed dynamics, and the goal of this thesis is to examine a paralympic wheelchair's dynamic performance. The performance analysis begins with a comprehensive literature review of several methodologies for quantifying wheelchair performance. Next, this research focuses on power measurement using a bicycle power meter constructed, fitted, and simulated on a paralympic wheelchair.

1.1. Background

Wheelchair racing has been an integral part of Paralympics and track racing since the mid-20th century. Its appreciation has grown immensely in the last 60 odd years since its inception in the summer Paralympics of 1960. The early years of wheelchair racing saw racers use heavy standard wheelchairs which were difficult to propel for long distances. Hence, they were never used for races beyond 200 meters (Cooper 1990, p. 296). The 1970s brought out the first modifications done to wheelchairs and the use of wheelchairs for specific sports (Cooper 1990, p. 296).

Wheelchair racing has changed dramatically since the late 1980s, with the design of the wheelchair finally shifting to the elongated, three-wheeled shape in the late 1990s. Due to significant modifications in both geometry and speed, wheelchair racing is a biomechanically distinct activity from propelling a traditional wheelchair. (Chenier et al., 2020.) Figure 1.1 shows how wheelchair racing was conducted during the first years since its inception.

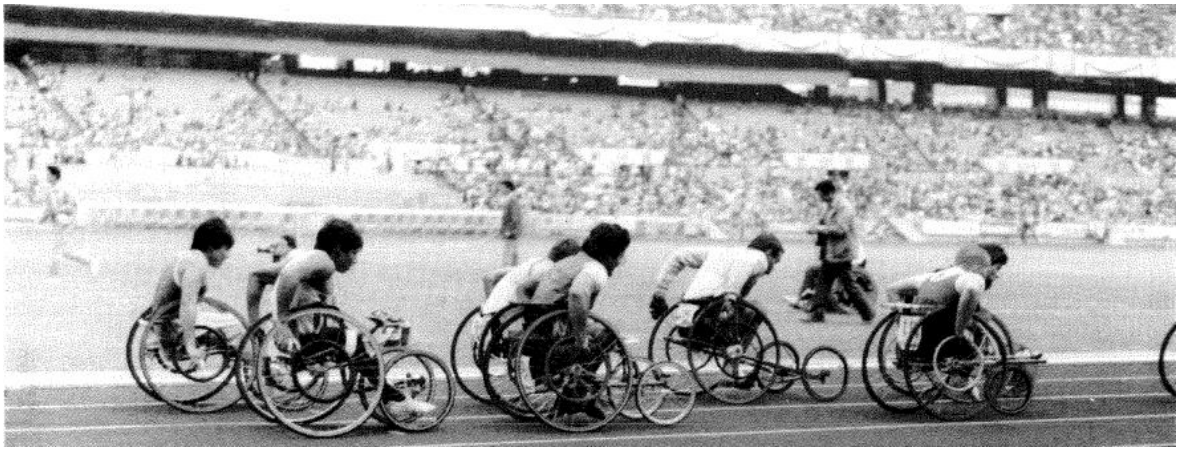

Figure 1.1. Wheelchair racing during early years (Cooper 1990, p. 296).

Wheelchair racing is frequently divided into categories based on the severity of disabilities, amputations, and spinal injuries, among other things. Wheelchair racing participants utilize specially manufactured wheelchairs that are not like those used by the general public. Figure 1.2 shows a modern racing wheelchair that is being used currently.

Figure 1.2. Modern Racing Wheelchair

Compared to 20th-century wheelchairs, modern wheelchairs are substantially safer, more unique, and speedier. Technology advancements have made them considerably more adaptable to each athlete's minute preferences. At least three wheels are necessary in modern

racing wheelchairs. The rear wheels can have a maximum diameter of 70 cm, but the front wheel(s) can only have a diameter of 50 cm. Only one push-ring is allowed on each rear wheel. Push-rings are typically 12 to 18 inches in diameter and are joined directly to the spokes by stand-offs. Faster acceleration is possible with larger diameter rings, but peak speeds may be reduced. Cambering the wheels provides the chair a bigger footprint, which improves stability. Camber also allows for a more natural straight-down push motion from the shoulders. However, too much camber can cause spoke stress and reduce wheel stiffness. Most users prefer a camber of 10°, but it varies amongst individuals from around 2° to as high as 12°.

Most modern racing seats are built of high-strength, low-density metals like chromium molybdenum alloy steel (chromoly), titanium, and similar materials. They have two huge, cambered back wheels and a smaller front wheel. The wheelchair's propulsion (or, to put it another way, basic mobility) comes from the back wheels. The athlete propels the wheelchair ahead using a push rim linked to both ends of the rear wheels. These push rims are usually made of lightweight materials like carbon fibre, just like the rest of the wheelchair, designed to be light and agile for easy movement. Athletes wear personalized gloves specific to each athlete and aid in rim pushing without producing friction.

1.2. Project objectives and research questions

The scope of this research is to determine how paralympic wheelchair athletes and teams may improve their performance by using a power meter. In addition, the study looks at how bicycle power meters can be fitted into in racing wheelchairs. There were no manufacturing techniques or practical trials in this study. Design for Manufacturing and Assembly (DFMA) principles were used in the design of the power meter assembly to ensure ease of assembly of various elements, however data on material usage, manufacturing costs, and maintenance costs were not accessible during the research and development phase. Figure 1.3 shows the primary goal of the thesis.

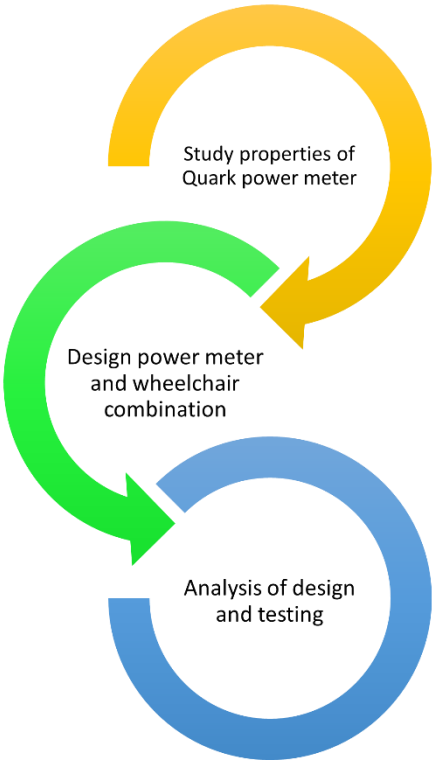

Figure 1.3. Aim of thesis

Objectives: The purpose of this thesis is to test the performance of a Paralympic racing wheelchair using the Quarq Dzero Dub Power Meter for a bicycle crankshaft. The power meter would be mounted on the wheelchair's back wheel, with considerable modifications to the push-rim and hub attachment. The objectives to be discussed from the design and simulation perspective are:

- Design the Quarq Power Meter and fit it around the rear wheel hub of the racing wheelchair.
- To analyze, discuss and interpret results obtained from the simulation results of the power meter attachment to the wheelchair.
- Compare the accuracy of results to the results of bicycle technology.

Research Questions:

1. How can the performance be quantified and improved?
2. Which is the best method to measure power?

3. How do we incorporate bicycle power measurement technology into racing wheelchairs?
4. How can the design corelate with real life application?

1.3. Methodology

The methods for this report will be organized in the manner depicted in the figure 1.4. Although, the solutions to the primary goal of power measurement in Paralympic wheelchairs were not practical due to complexity, inaccuracy, costs, and weight, such as strain gauges, force measuring gloves, and bespoke push rim are investigated first. In doing so, the study examines various ways that cannot be properly implemented but are still important in understanding the research's limits.

The current study strategy involves taking technology from bicycles and putting it into wheelchairs. This technology transfer necessitates a thorough examination of the technical implications while developing the power meter assembly. In Chapter 5, the study's important conclusions will be determined by reviewing the design and the estimated accuracy of the results obtained and discussing the limiting variables. In addition, the conclusion summarizes the research's main findings and discusses prospects. The methodology is given graphically in figure 1.4.

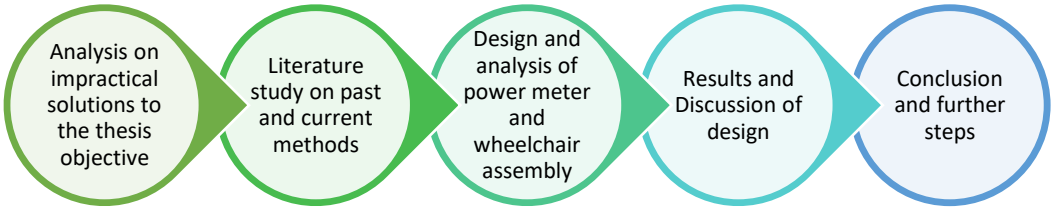

Figure 1.4. Methodology

2. Literature Review of power measurement approaches

Any new product or technology concept necessitates some investigation into past methodologies and studies related to the subject. It's critical to comprehend the research's limitations and previous approaches to the topic. The outcomes of previous studies can be used to develop new ways and push the boundaries of study and experimentation. In this situation, earlier studies and attempts to measure power in wheelchairs aid in identifying the technological limitations of such methodologies and improving or revolutionizing power measurement methods. These include the idea of using simple Wheatstone bridge-based strain gauges, the novel concept of a Tactile Glove, and previous attempts to create a custom instrumented push rim to measure the athlete's power, which were not used in the final solution because they did not address our research problem.

2.1. Previous approaches in power measurement

This chapter focuses on evaluating prior attempts to quantify power in this thesis and understanding why they failed. The importance of examining these failed attempts is to better understand the research and experimentation that led to the present power measurement system, which includes embedding the quarq power meter into anything from bicycles to wheelchairs.

2.1.1. Strain Gauges

Strain gauges measure the amount of strain applied to an item. Strain gauge measurements are widely used in many industries. Using proper measurement instruments, the strain level in numerous constructions, from biomechanics to civil engineering, may be defined. (Tutak,

2014, pp. 135-145.). The strain gauge measurements include force, deflection, pressure, flow and is employed by all facets of engineering for various purposes as shown in the figure 2.1.

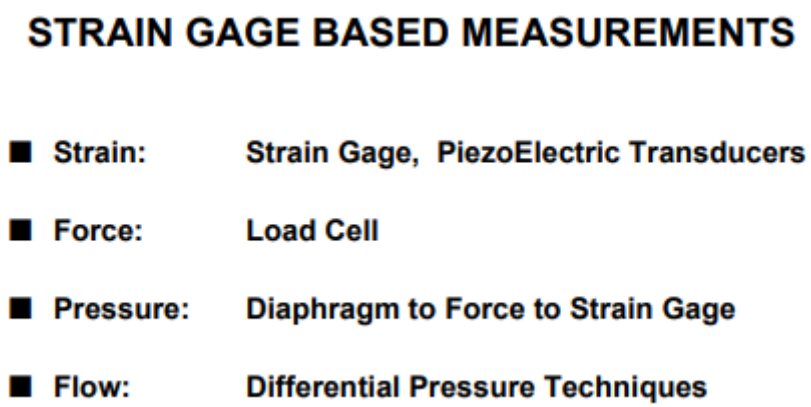

Figure 2.1. Strain gauge-based measurements, (Kester, 1999).

The strain gauge concept was idealized and used in this study to measure force to measure the performance of the Paralympic athlete. As Kester (1999) said "The strain gauge measures force indirectly by measuring the deflection it produces in a calibrated carrier". The typical strain gauge construction is shown below in figure 2.2.

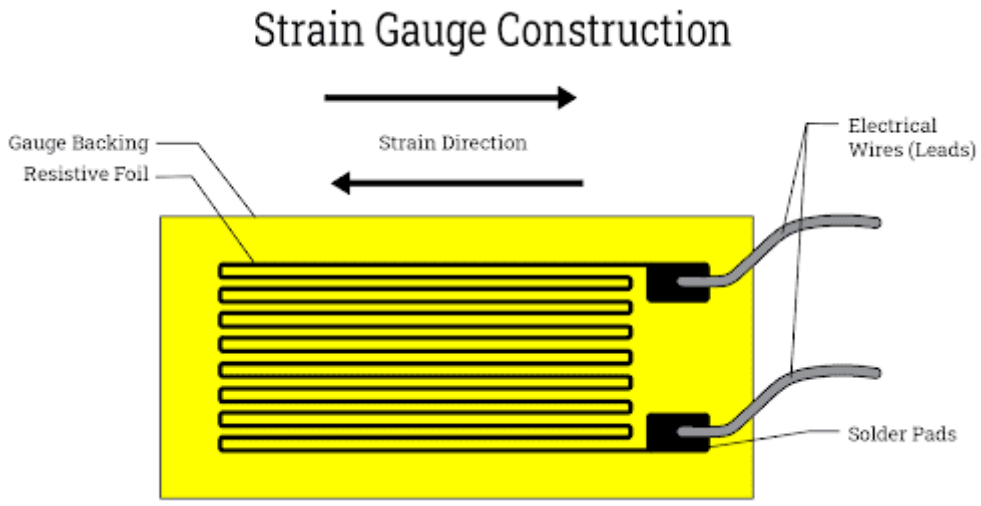

Figure 2.2. Strain gauge construction, (IQS Directory, 2011).

It consists of a long, thin conductor attached to an elastic supporting material called a carrier. When the size of a conductor changes, so does its electrical resistance. (IQS Directory, 2011). Strain gauges measure force using the Wheatstone bridge principle. A Wheatstone bridge is a four-resistive-element electrical circuit (Tutak, 2014, pp. 135-145) shown in figure 2.3.

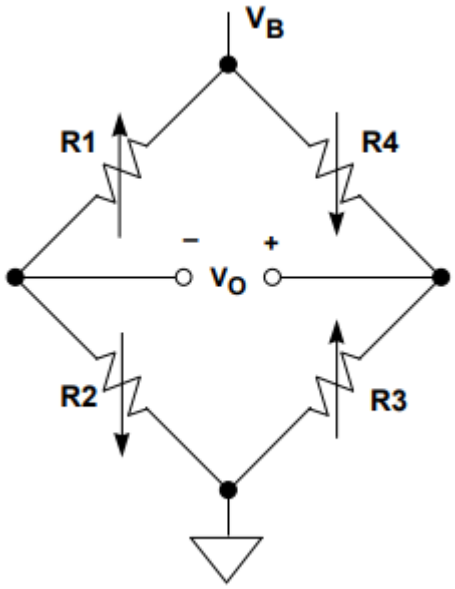

Figure 2.3. Wheatstone bridge, (Kester, 1999).

The bridge works on the voltage divider rule. As a ratio of the matching bridge resistances, whenever a supply voltage is given to the two bridge supply points 2 and 3, it is split into two halves of the bridge R1, R2, and R4, R3, forming a voltage divider in each half of the bridge (Hoffmann, 2012).

In general uses, strain gauges can be used to measure force applied on flat beams by placing two gauges on each side of the beam so that it measures the deflection from both sides. An example of this configuration is shown below in figure 2.4.

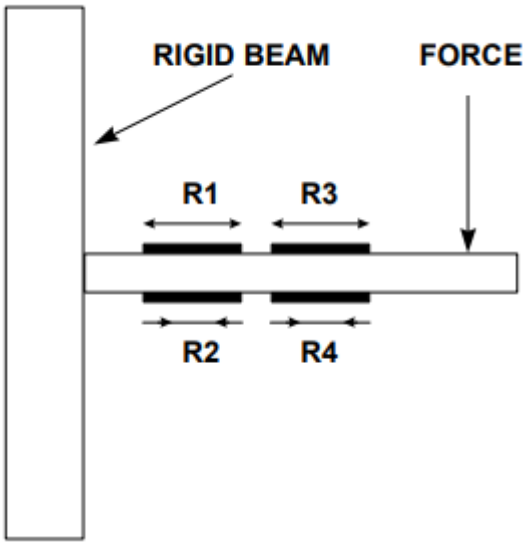

Figure 2.4. Strain Gauges on a flat beam, (Kester, 1999).

The figure made by Kester (1999) shown above has a horizontal beam attached to a vertical rigid beam on the left and undergoes a force application on the right end. The strain gauges are placed in the form of the Wheatstone bridge on either side to ensure equal voltage division.

These strain gages can detect even the tiniest deflections. The strain caused by the force application is estimated in this use case to see if the strain can be measured effectively if the gages are situated correctly. This computation is performed with the push rim cylindrical rather than rectangular.

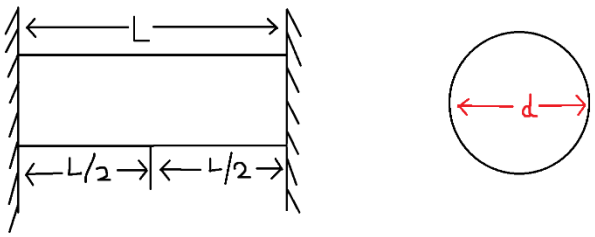

$$M = wl/8 \tag{2.1}$$

In equation 2.1, M is the moment in [Nmm], w is the work done in [N] is equal to 425 N, l is the length of clamp in mm and is equal to 13 mm. Therefore, the moment is 690.6 Nmm.

$$z = (\Pi\, d\text{^}3)/32 \tag{2.2}$$

In equation 2.2, z is the section modulus in [mm^3], d is the diameter of the section in [mm] and is equal to 5mm. Therefore, z = 12.27 mm^3.

$$\varepsilon = M/ZE \tag{2.3}$$

In equation 2.3, ε is the total strain and E is the Young's Modulus of aluminium [N/mm^2] which is the material used and is equal to 69e3 N/mm^2. Therefore, the value of strain that is applied on the push rim clamp of the wheelchair is 0.0008. This value of strain is measurable using standard 2x2 or 2x3 strain gauges. Also, the strain gauges must be connected to other data processing devices which have to be mounted on the wheelchair to gather data. These can be mounted near the centre of the wheelchair, a.k.a, hub.

2.1.2. Tactile Gloves

The ergonomics of a Paralympic wheelchair is remarkably interesting and requires precision to unlock the maximum potential of the athlete. Wheelchair racing aims to achieve highest acceleration in the shortest possible time. Hence, the propulsion forces applied by the athlete play an instrumental role in his/her performance (Forte et al., 2015). The high acceleration is achieved by repeating the propulsive movements by repositioning the hands on the push rim to perform another propulsion cycle (Barbosa and Coelho, 2017). The CAD model of the propulsion cycle is shown in figure 2.5.

Figure 2.5. CAD model of a complete propulsion cycle (Forte et al., 2018).

The successful multi-cycle wheelchair movements require consistency and durability, from both the athletes and their equipment. A primary piece of equipment crucial for a rider's success is the racing gloves. The racing gloves are bespoke and customized to every rider's hand to aid ergonomic use of the push rim. Wheelchair racing gloves are solid 3-D structures clutched in a clenched fist that help move the wheelchair forward by pushing the glove against a revolving rail linked to the wheel (Covill et al., 2020). There are currently many glove sizes to fit all fist shapes and sizes. However, there has recently been a push to make custom-fit gloves using 3-D scanning technology. A common type of racing glove is shown in figure 2.6.

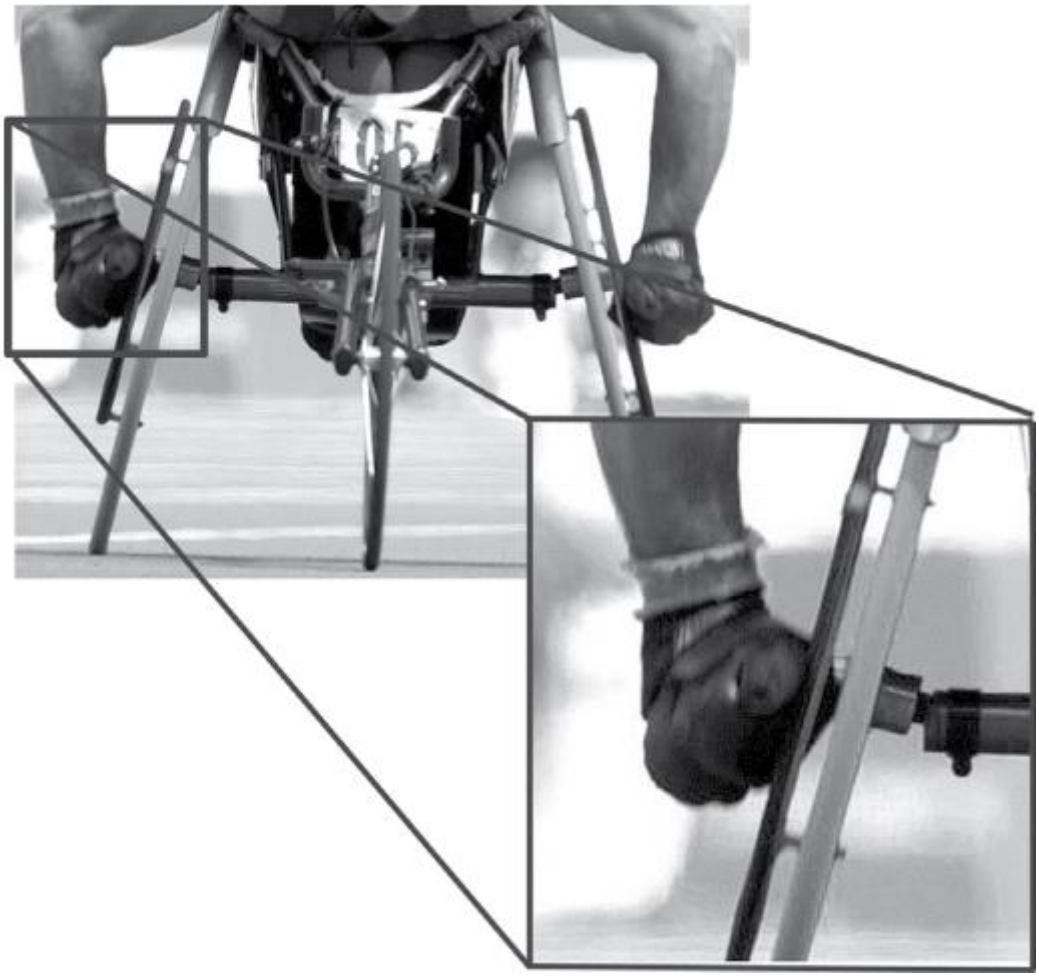

Figure 2.6. Soft racing gloves (Rice et al., 2015).

This study aimed to employ strain gages to assess the force that the athlete applied through the gloves. Therefore, understanding how pressure sensors in gloves work to utilize this technology was required. TactileGlove is a device with pressure sensors embedded in the gloves' fabric that gathers natural pressure mapping data to better comprehend diverse hand interactions. (Pressure Profile, 2020.). “Nearly any hand interaction and operation can be quantified accurately with the TactileGlove” (Pressure Profile, 2020). Figure 2.7 shows the interior of the TactileGlove with the sensors attached.

Figure 2.7. Inside view of TactileGlove (Pressure Profile, 2020).

The sensors shown in figure 2.7 transmit data to a software called Chameleon which reads the data and delivers numerical results. The table 2.1 shows the technical specifications of the tactile glove. The user interface of the software is shown in figure 2.8.

Table 2.1. Technical specifications of TactileGlove sensors (Pressure Profile, 2020).

Sensing Elements	65
Full scale range	80 psi (55 N/cm^2)
Maximum Force	Thumb & Fingertips – 70 N Pinky Tips – 28 N
Thickness	2.6 mm (approx)
Signal to Noise (SNR)	>500.1
Gain Non-Repeatability	<3%
Linearity	>98%
Minimum Sensitivity	0.04 N
ELECTRONIC SPECIFICATIONS	
Scan Rate	25-40 Hz
Interconnection	Wireless Bluetooth Low Energy (BLE) – minimum 5m range
Battery Life	>2hrs
Operating Temperature	0-50^o C

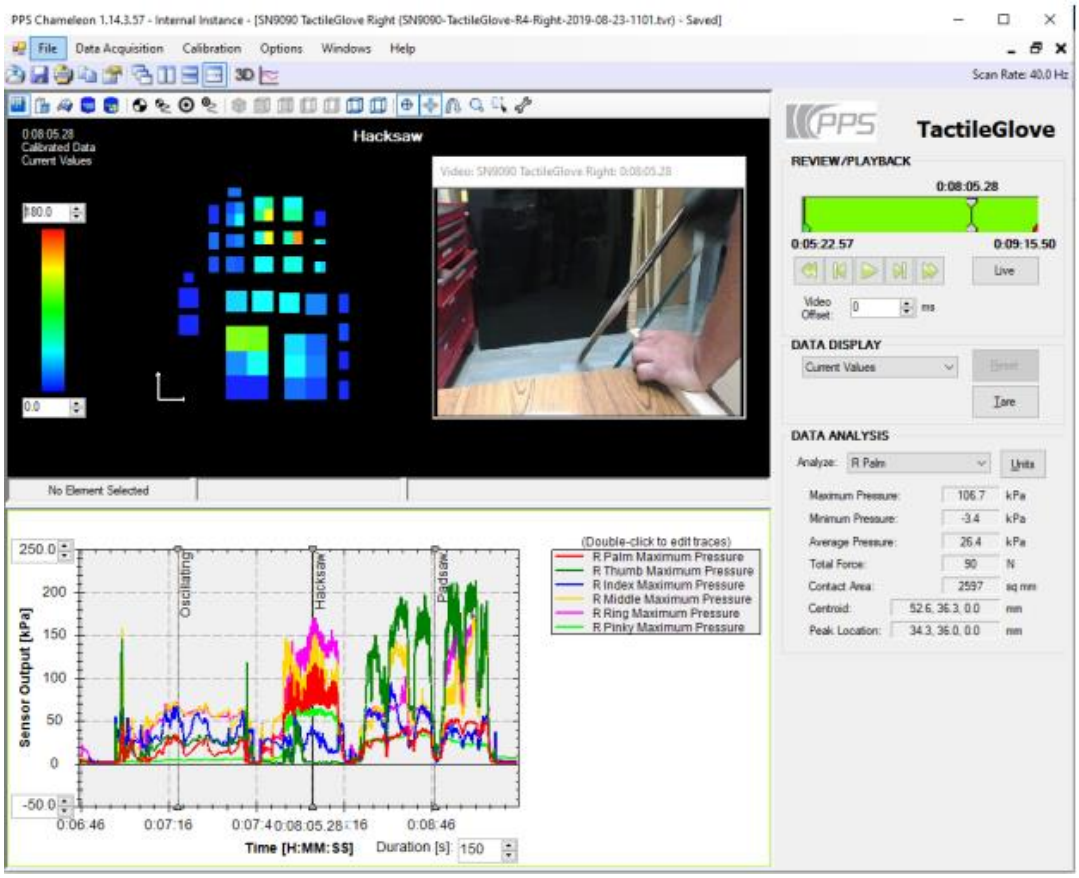

Figure 2.8. Example data captured by the glove while sawing wood (Pressure Profile, 2020).

The glove detects a pressure spike during the operation with the oscillating saw, which is created by pushing a firm on/off sliding switch. The force is directly measured and presented in Newtons, as seen in figure 2.8.

2.1.3. Custom Wheelchair Push Rim

A racing wheelchair's propelling strategy and performance are vastly different from that of a standard wheelchair (Miyazaki et al., 2020). In simple terms, the performance of the wheelchair is how fast and how efficient is the racing wheelchair. To ensure accuracy and that the dynamics of the wheelchair is not disturbed significantly, exploring the possibility of developing a custom push rim was initiated in this thesis study. This task's feasibility

requires the relationship between propulsion motion and aerodynamic drag, which can fluctuate throughout propulsive motion, to be established (Miyazaki et.al, 2020).

Chénier et al. (2020.) stated that “There is currently no instrumented racing wheel that can wirelessly and at a high sample rate capture 3-D push rim kinetics”, which is required for reliably evaluating wheelchair racing biomechanics. However, it is possible to develop a custom push rim with fitted instruments. Miyazaki et al. (2020.) said that “because individual athletes' racing wheelchairs are optimized in terms of sheet position and push rim diameters, a push-rim force measuring device for individual athletes' racing wheelchairs is needed”, as well as clarification of the relationship between propulsive style and output of push-rim forces, which change for each athlete. Therefore, they developed a custom instrumented push rim mounted on to the wheelchair and is evaluated in a wind tunnel facility to measure the air drag which also plays a huge factor in determining performance of the wheelchair. The force sensor system is shown below figure 2.9.

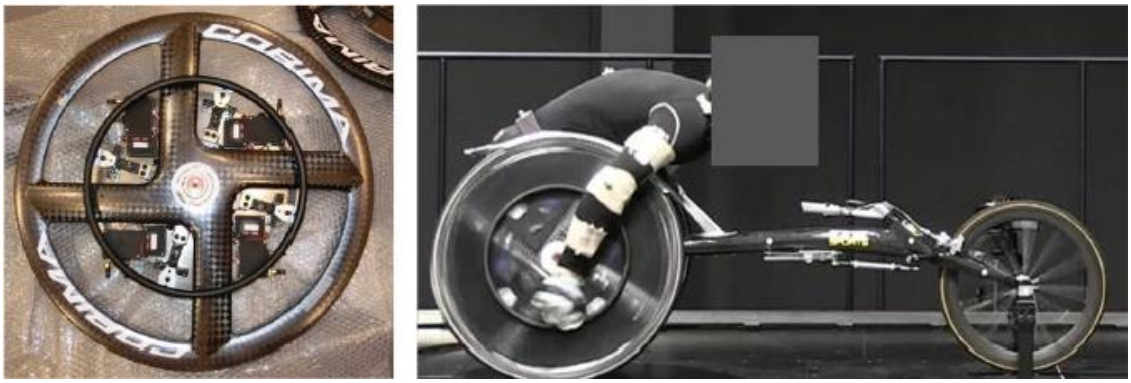

Figure 2.9. Force sensor system (Miyazaki et. al, 2020).

Similarly, Limroongreungrat (et al., 2009.) also designed and validated an instrumented wheel system which measured the pushrim forces. The instrumented wheel system as indicated in the figure 2.10, included a 3-D JR3 force transducer, an interface plate, a rear wheel, a push rim, and a slip-ring unit

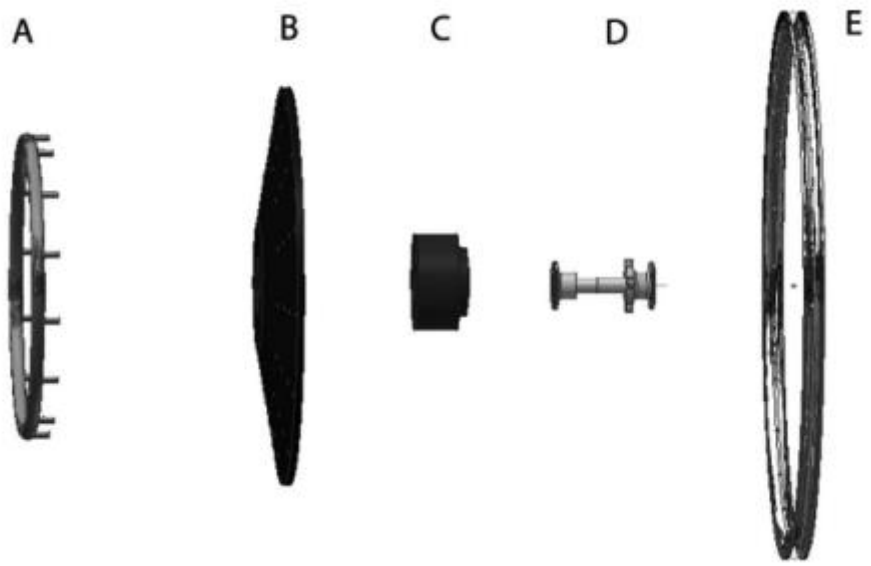

Figure 2.10. Instrumented Wheel System parts (Limroongreungrat et al., 2009).

Fitting four 2-D component force sensors, batteries, and radio transmitters to be able to read the data on a computer met the athletes' needs in the supplied study. The usage of strain gauges is further highlighted in this case study. The sensors were made of duralumin and mounted with 4x3 strain gauges to detect the force sensors readings on the push rim. The Wheatstone bridge principle was used to construct the strain gauge reading structure. In contrast, 4x2 strain gauges were used to quantify the tangential and radial forces of the push rim. The wheelchair push rim's ergonomics and the time settings are shown in figure 2.11.

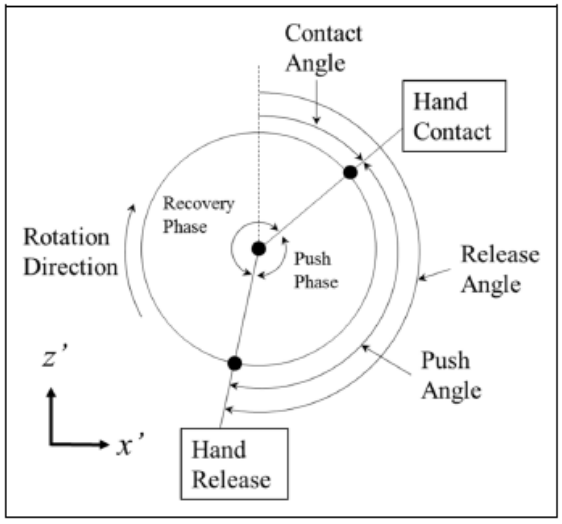

Figure 2.11. Stroke cycle (Miyazaki et al., 2020).

Three trials with three different athletes were used in this investigation. The outcomes were consistent, and the 2-D forces measured by the strain gauges demonstrated that the measurements were accurate. However, the inaccuracy range of the force sensors inside the push rim is between 0-2.4 percent, according to the measurements. The forces measured at various angles where the sensors were monitoring the forces are shown in table 2.2.

Table 2.2. Results of calibration tests under 500 N static load (Miyazaki et al., 2020).

Sensor Mounting Position (º)	**Loading Position (º)**	**Measured Load**		**Error (%)**	
		F_x (N)	F_y (N)	F_x	F_y
0	0	1.0	-504.1	0.5	0.8
	90	1.0	-500.6	0.3	0.1
	180	-2.2	-500.6	-0.4	0.1
	270	1.0	-505.7	0.2	1.1
45	0	348.2	-353.3	-1.5	0
	90	350.1	-355.1	-1.0	0.4
	180	345.1	-352.7	-2.4	-0.2
	270	349.9	-352.3	-1.0	-0.3

90	0	497.3	2.0	-0.5	-0.4
	90	489	-0.5	-2-2	0.2
	180	497.1	-2.2	-0.6	-0.4
	270	490.2	0.1	-2.0	0.2
135	0	345.7	350.4	-2.2	-0.9
	90	349.9	353.3	-1.1	-0.1
	180	346	350.4	-2-2	-0.9
	270	350.4	354.7	-0.9	-0.3
180	0	1.6	502.1	0.3	0.4
	90	1.2	501.9	0.3	0.4
	180	2.6	501.5	0.5	0.3
	270	2.0	496.7	0.4	-0.7
225	0	-346.2	353.2	-2.1	-0.1
	90	-347.8	353.7	-1.7	0
	180	-347.3	355.8	-1.8	0.6
	270	-348.4	355.6	-1.5	0.6
270	0	-496.2	0.7	-0.8	0.5
	90	-494.1	2.1	-1.2	-0.5
	180	-497.2	2.0	-0.6	0.4
	270	-490.4	-1.1	-1.9	0.4
315	0	-345.1	-356.9	-2.4	0.9
	90	-351.2	-353.7	-0.7	0
	180	-345.9	-352.4	-2.2	-0.3
	270	-347.1	-353.2	-1.8	-0.1
Average Error				1.2	0.4

2.2. Power measurement in wheelchairs

Performance analysis has multiple facets, i.e., power measurement, velocity, angular displacement, stress, strain, etc. However, the most critical aspect of performance analysis in racing is power measurement. When driving through terrain, rolling resistance, bearing resistance, tire scrub, and other frictional components like drag and frame bending all contribute to resistive energy losses. In sports like cycling and wheelchair racing, power measurement is an important performance parameter, since it is less sensitive to variations in wind and road conditions. (Pelland-Leblanc et al., 2014.)

A power meter, used in cycle sports is a device used to measure the power input of a rider. It is primarily used to measure and improve performance of a bicycle rider in terms of Watts. (Mcainsh, 2014.) The power meters have been increasingly popular during the last decades as the importance of athletes' performance grows. In recent history, the use of power meters to measure athletes' performance in multiple sports, albeit, not in Paralympic sports, have increased significantly. The most common types of power meters existing today use strain gauges to measure torque. Power is usually measured at the crankset or hubs of the bicycle, which is what companies like Quarq, PowerTap and Garmin Vector use. (Fuglsang, 2015.)

The power measured is in Watts in cycles which is defined as work done in each period. Mathematically, it is represented as:

$$P = \Delta w / \Delta t \tag{2.4}$$

where P is the power [Watts], ΔW is the change in work and Δt is the change in time. (Fuglsang, 2015) Furthermore, the PO assessment can be utilized in a variety of studies to quantify the impacts of rehabilitation programs or to assess the level of fitness improvement generated by medical treatments, recovery strategies, and a variety of other ways. (Bouillod et. al 2022 p. 1; Isacco et. al 2016, Pp. 1204-1207; Majerczak et. al 2017, Pp. 70-85; Menetrier et. al 2013, Pp. 49-56.)

The focus for this project is to use the technology developed for bicycles and apply it to racing wheelchairs. As always, the direct transfer of technology from one domain to another involves a lot of complications and that it what this thesis aims to solve. (Forte et al., 2015) To achieve this successful transfer of technology, it is imperative to identify the correct locations to fit the power meter into the wheelchair by looking at the validity of each area. Figure 2.12 depicts the several areas where a power meter can be mounted on a bicycle.

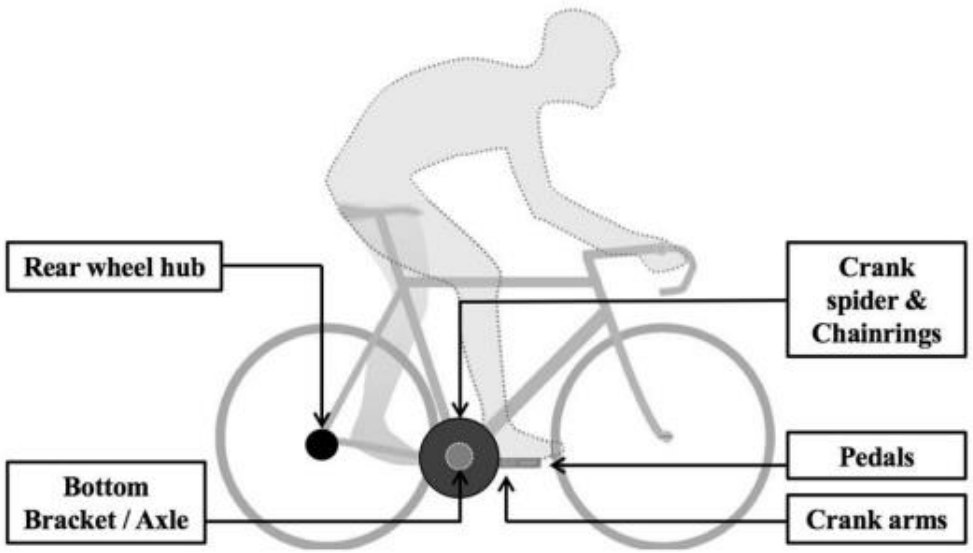

Figure 2.12. Power meters' location on the bicycle Stroke cycle (Bouillod et al. 2022, p. 3).

According to Bouillod (et al., 2017, p. 1023), the maximum PO would be measured at the pedals, while the lowest PO would be obtained at the rear hub due to mechanical losses in the bicycle components. The specifications of the quarq power meter for the use in paralympic wheelchairs are shown in table 2.4.

Table 2.3. Quarq power meter specifications

Parameter	***Value***	***Units***
Weight	125	grams
Bolt Circle Diameter	110 or 130	mm
Accuracy (Approx.)	+/- 1.5	Percent (%)

Battery Type	CR2032	-
Battery Life	200	Hours
Software	ANT+ / Bluetooth	-

The quarq dzero dub power meter is preferred over other power meters in this category for the application into the wheelchair. Although most power meters available in the market today do measure power accurately according to the locations they are fitted onto. A study conducted by Miller (et al., 2015) shows that variations in power assessments between power meters may be attributed to cadence measuring ability, despite strong agreement during steady riding. Figure 2.13 demonstrates that the relative frequency of the quarq power meter, depicted by a white bar, is higher or almost equal to that of the Stages power meter and the Powertap power meter, respectively.

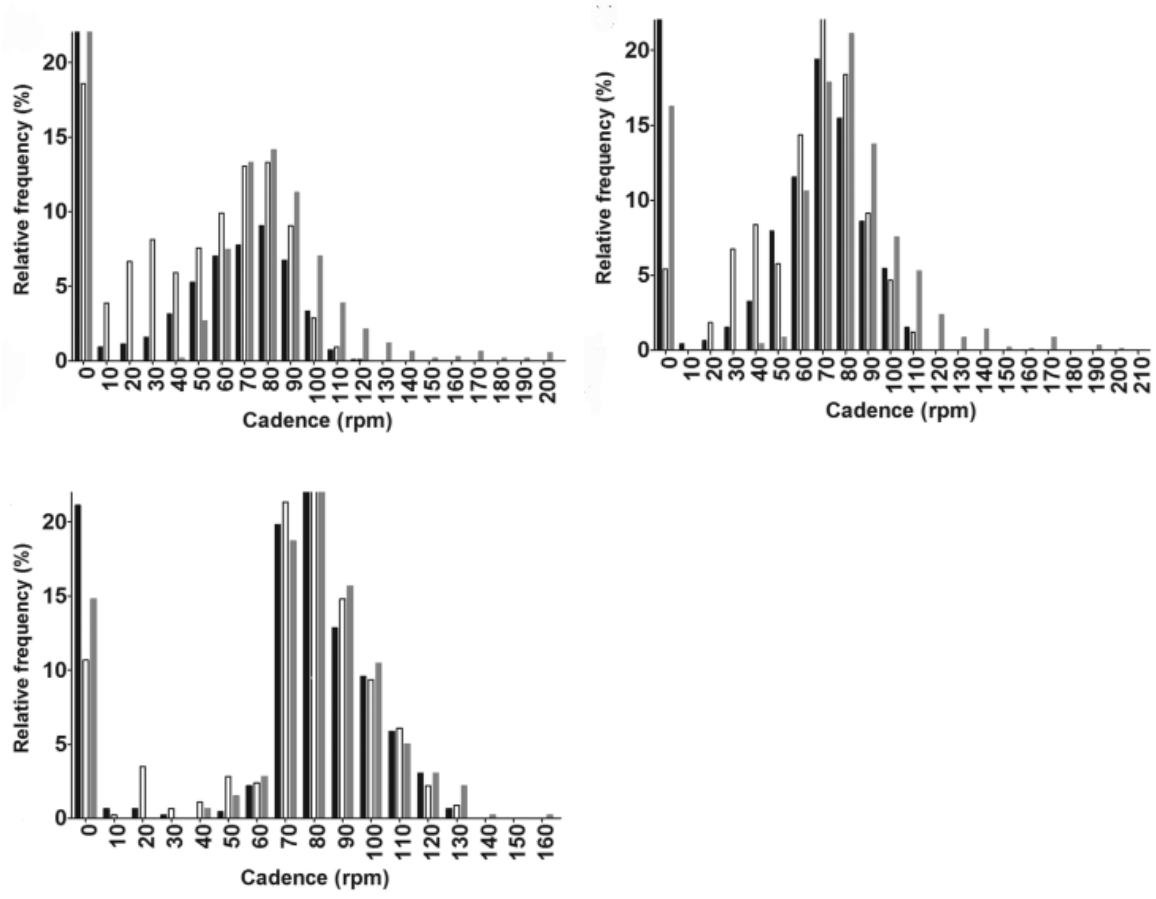

Figure 2.13. Cadence measured when cycle goes (a) Downhill (b) Flat line (c) Uphill (Miller et al. 2015, p. 7).

The second and more important reason for incorporating the quarq power meter into the paralympic wheelchair is that it is perfectly designed and fitted to the paralympic wheelchair, albeit with some changes. Furthermore, the quarq power meter is lightweight and has no impact on the paralympic rider's stability or weight distribution in the wheelchair. In addition, the quarq power meter eliminates the need for maintenance, which is critical for long-term use.

The power meter is most typically found on the hub of a bicycle, and this study tries to apply it to a paralympic wheelchair. The quarq power meter is attached to the bicycle's crankset. Figure 2.14 shows a schematic diagram of an example power meter.

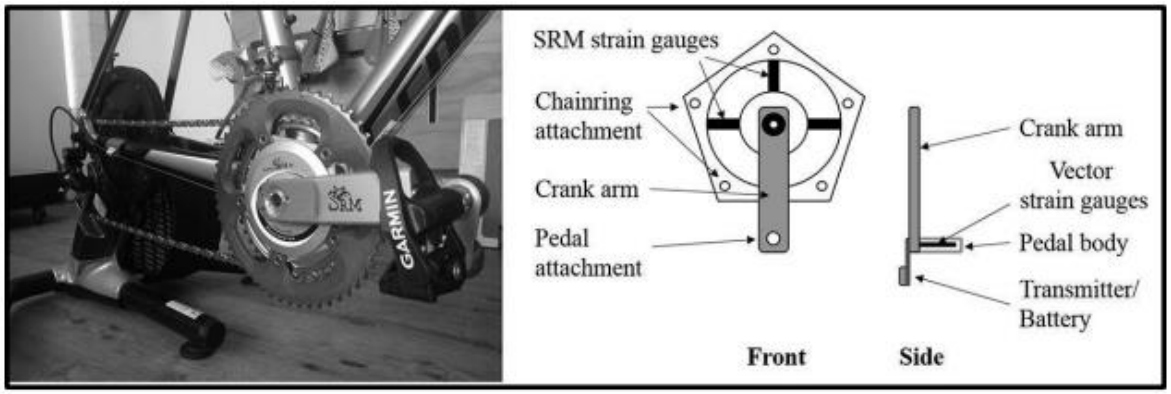

Figure 2.14. Stationary bicycle fitted with crank power meter made by SRM (Daniels 2017, p. 10).

As the figure shows, the power meter is rigidly attached to the crank arms and the chassis of the bicycle. The power meter detects the force applied to the pedals of the bicycle radially using strain gauges lined in a circular pattern and mounted on the back of the power meter. The strain gauges monitor the applied pressure, which is then converted to torque, and the output of the measured parameter is transmitted to a computer or another compatible power device via the ANT+ program.

The power measured in this use case is given by the mathematical formula:

$$P = \tau * C \tag{2.6}$$

In equation 2.6, P is power applied [Watts]. The torque is given by τ in [Nm] and C is the cadence (or) the angular velocity of the object and is represented in [m/s]. Figure 2.15 shows the location where the strain gauges are fitted on the quarq power meter.

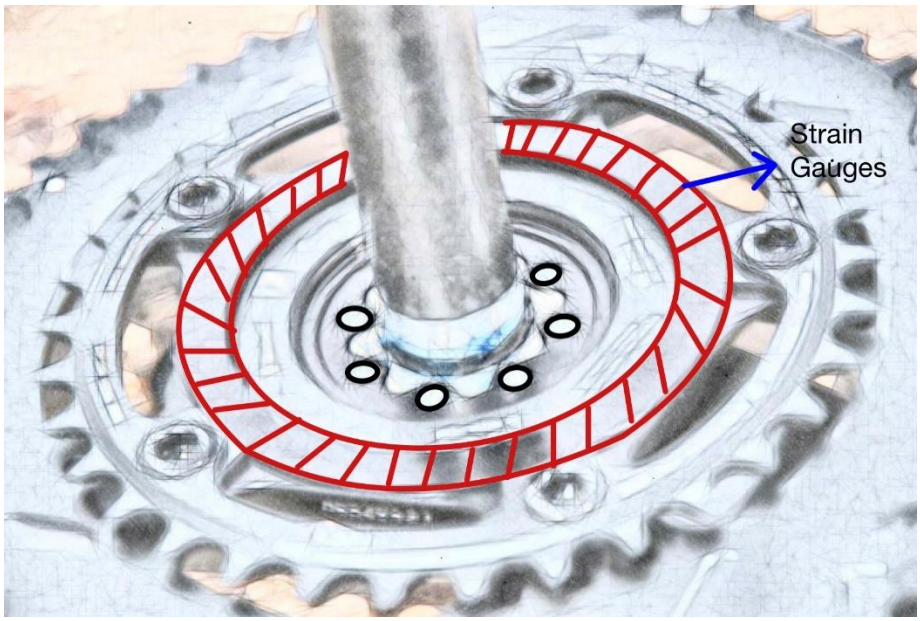

Figure 2.15. Strain Gauge alignment on Quarq dzero power meter

ANT is a proprietary protocol created for applications that demand long-term monitoring while consuming little power. It divides its bandwidth into 125 channels, each with a 1MHz width, and runs at 2.4GHz with a transmission time of fewer than 150 microseconds per frame for 8bytes of data. It distinguishes between networks using unique network keys. (Mehmood and Culmone, 2015, p. 3.)

In this case, the ANT+ program enables users to read the data collected by the power meter in a simple manner. Any computer having the ANT software can connect to the power meter which has a transmitter built-in and relays information to the software. The ANT software decodes this information and displays the power output to the user in terms of Watts.

2.3. Paralympic Wheelchair Dynamics

This chapter focuses on identifying and researching essential elements of wheelchair dynamics, such as a racing wheelchair's overall functionality, which provides insight into the biomechanics of wheelchair propulsion and illustrates the forces operating on the wheelchair's push rim. The power meter designed in Chapter 3 will be used to record and measure these forces.

2.3.1. Dynamics of wheelchair

The motion of bodies under the influence of forces is the subject of dynamics. It can also be defined as the study of mechanics related to motion and/or equilibrium. In the context of wheelchair racing, dynamics refers to the science of the paralympic wheelchair movement along a path. Starting, accelerating, Steady State wheeling, and sprinting are the distinct movement dynamics in wheelchair racing (Vanlandewijck et al. 2001, p. 356). Wheelchair propulsion is a meticulous process that requires extensive training. The propulsion phase and the recuperation phase are the two key phases of the wheelchair stroke. The stroke cycle is further divided into five stages: catch, drive, release, lift and stretch, and acceleration (Forte et al., 2015). A typical stroke cycle is shown in figure 2.16.

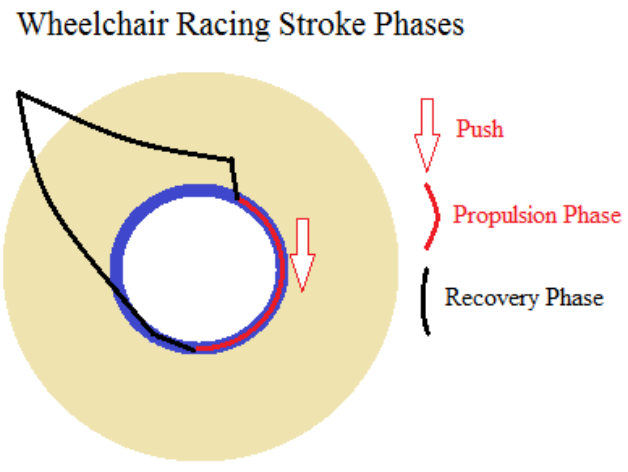

Figure 2.16. Stroke cycle in paralympic wheelchair racing (Forte et al., 2015).

Wheelchairs, as mentioned in Chapter 1, have progressed over the last few decades in terms of design, handling, and efficiency. When a wheelchair user's physical and functional capacity improves as he or she moves from a rehabilitation patient to a competitive athlete, however, wheelchair performance improves. Furthermore, considerable advancements in wheelchair concepts and wheelchair athlete interface have improved performance (Vanlandewijck et al. 2001, p. 356). Figure 2.17 shows the comparison in seating position and propulsion characteristics of a 1986 paralympic wheelchair and a modern counterpart.

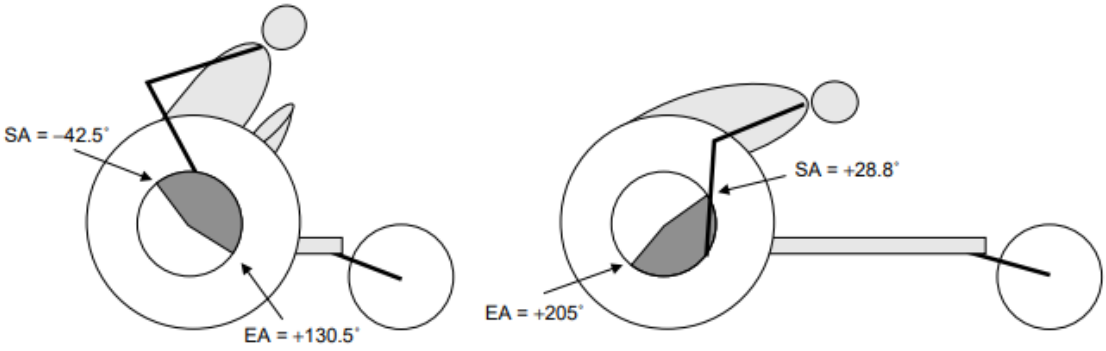

Figure 2.17. Comparison of a 1986 wheelchair (left) and a 1995 wheelchair (right) (Vanlandewijck et al., 2001, Higgs, 1986).

Compared to previous wheelchairs, the modern wheelchair has a lower hand placement and a more aggressive seating position, as shown in figure 2.17. This is primarily due to the wheelchair's new elongated shape, which improves stability, control through turns and at high speeds, and the athlete's overall performance.

The paralympic athlete's hand posture is critical for a good launch from a stationary position. The athlete should place his hand at an angle more than 90 degrees to the horizontal when launching. When it comes to evaluating an athlete's performance, biomechanics of the

wheelchair is crucial. A study done by Sanderson and Summer (1985.) iterates that the hands are in touch with the push rim, allowing the muscle force to sustain or enhance the wheelchair's pace. The propelling phase begins when hands hold the push rim near or behind top dead center, TDC. This phase will end when the hands are released from the push rim. Hands are released from the push rim during the recuperation period, the grip is retaken, and a new propulsive phase begins. In theory, this occurs, although it is not as evident as the circular technique. Higgs (1993) described the five-step cycle as the acceleration phase, the energy transfer phase, the drive phase, the rotation phase, and the disengagement phase shown in figure 2.18.

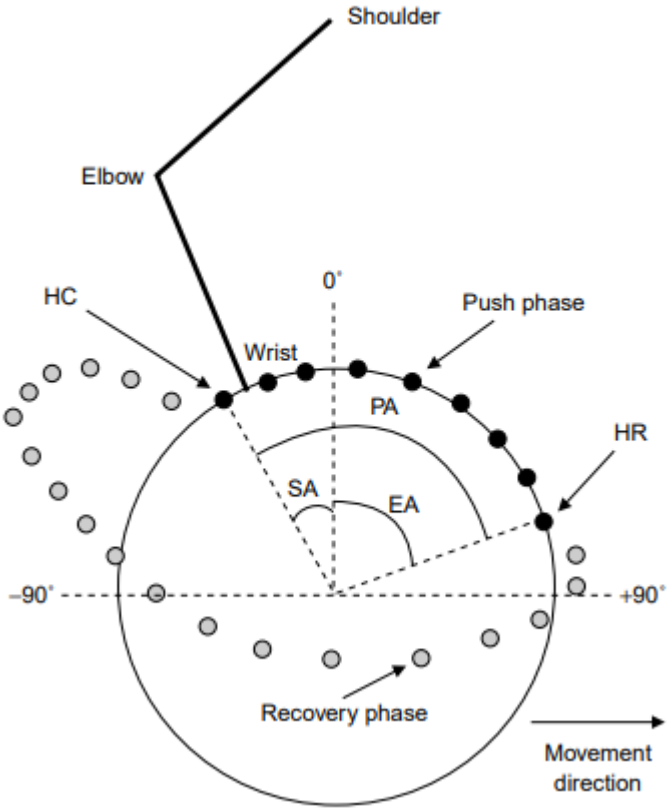

Figure 2.18. Wheelchair propulsion technique: HC- hand contact, HR – Hand release, SA – start angle, PA – push angle, EA – end angle (Vanlandewijck et al., 2001).

2.3.2. Forces on a wheelchair

“Improving wheelchair propulsion has spawned a wide body of research, including inertia and resistive loss studies of mechanical systems and components.” (Thacker and Foraiati, 1991; Van der Woude et al., 2003; Lin et al., 2015)

A paralympic wheelchair is subjected to a variety of forces. The most significant force application is the athlete's force on the wheelchair's push rim. Therefore, push rim force measurements are crucial for evaluating an athlete's performance. The kinematics of wheelchair system, which were examined in Chapter 2.3.1, determine the magnitude of this force or torque produced by the athlete.

The precise measurement of 3-D pushrim reaction forces could predict wrist, elbow, and shoulder joint reaction forces during wheelchair racing. These projections could lead to a better understanding of damage mechanisms, allowing for improved or modified racing wheelchair propulsion tactics and a reduction in the likelihood of upper extremity joint damage. (Limroongreungrat et al. 2009, p. 183.)

Limroongreungrat (et al. 2009, p. 183); Asato (et al. 1993); Finley (et al. 2004); Wu (et al. 1998.) believe biomechanical study will uncover the causes and effects of high upper extremity stress during traditional wheelchair propulsion. Although researchers have spent the last two decades studying the kinematic and kinetic features of standard wheelchairs and various sport/recreational wheelchairs, direct measurements of the push rim reaction forces during racing wheelchair propulsion remain uncommon.

This is primarily due to the complex anatomy of modern wheelchairs and the lack of reliable references through which an attempt to measure the push rim forces can be made. As Robertson et al. (1996.) emphasizes, there is no information on the forces applied to the push rim or the forces exerted across the joints during wheelchair propulsion, making it difficult to construct a reliable system for measuring them. Forces applied to the push rim have been measured using static force measurements, external devices such as force plates and

connections to isokinetic dynamometers, and direct push rim forces using various types of force measuring transducers. However, few of these studies have directly measured push rim forces while people pushed commonly used wheelchairs.

The forces exerted on the push rim are not parallel to the ground. As a result, the forces are split into two parts: a radial component, F_r, and a tangential component, F_t. The tangential component is the direction in which actual force is put on the push rim, and it is essential for assessing the athlete's performance. The force components and are shown in figure 2.19.

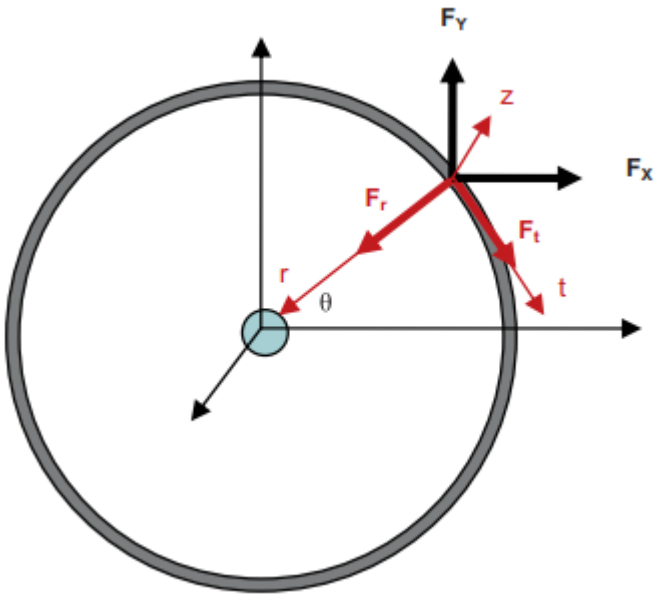

Figure 2.19. Force components on push rim (Limroongreungrat et al. 2009, p. 187).

The push rim forces are not the only forces considered when assessing performance of the wheelchair or athlete. Drag forces play a vital role in wheelchair racing dynamics. Drag is defined as the force resisting the movement of any object and occurs when the object (solid) interacts with a fluid medium (liquid or gas). Drag force can be generated from any part of the object unless they are aerodynamically sound. “Rolling resistance, bearing resistance, tire scrub, and other frictional elements such as drag and frame flexing all contribute to resistive energy losses when moving over terrain” (Caspall et al., 2013; Brubaker, 1986; Lin et al., 2015.).

In wheelchair racing, there are two types of drag forces: rolling resistance and aerodynamic drag. Rolling resistance is the drag force applied to the ground against the direction of motion of the wheelchair due to friction between the tyres and the ground. When a wheelchair is in motion, it is subjected to aerodynamic drag, caused by air resistance. Figure 2.20 shows the free body diagram of the wheelchair in the propulsion and recovery phase.

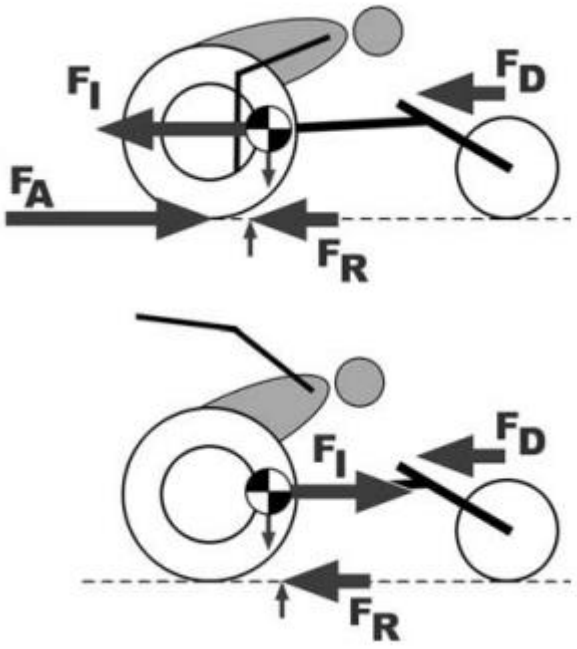

Figure 2.20. Free body diagrams of propulsion phase (top) and recovery phase (bottom) (Fuss 2009, p. 42).

The rolling friction force in wheelchair racing can be altered by lowering the equipment's bulk. Because of the lower rolling friction force and higher accelerations caused by mass reduction, higher velocities are generated, increasing drag force. (Fuss 2009, p. 43) Coutts (1991, p. 48.) conducted an experiment where a subject conducted multiple trials coasting on a downwad wooden floor in a sport wheelchair. The velocity ranging from 4.6 km/h to 19.1 km/h indicates that the increase in drag at higher velocities occurs with any type of wheelchair in multiple environments. The figure 2.21 shows the relation between drag force and velocity.

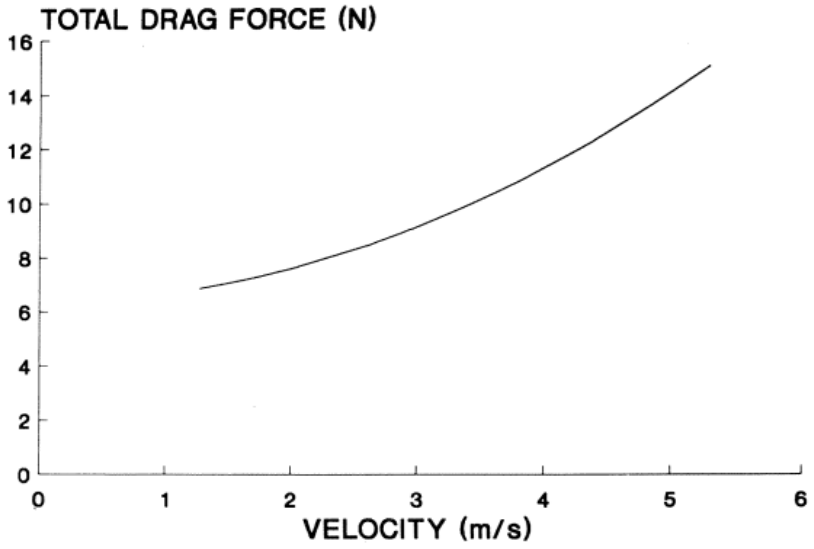

Figure 2.21. Drag force versus velocity in a wheelchair (Coutts 1991, p. 48).

The drag forces, as important as they are for total wheelchair performance, are not investigated extensively in this thesis since the focus is on the push rim forces and how they may be approximated when the force travels to the paralympic wheelchair's hub.

2.4. Design and analysis of wheelchair power meter

Engineering design is a method used by engineers to create a useful product or process. Figure 2.23 depicts the machine design rules used around the world, of which this thesis makes use of a few. For example, the concept of the power meter assembly shown in figure 3.1 was created using six engineering design concepts shown in figure 2.22. In addition, a brief overview of the Finite Element Analysis (FEA) investigation will be provided.

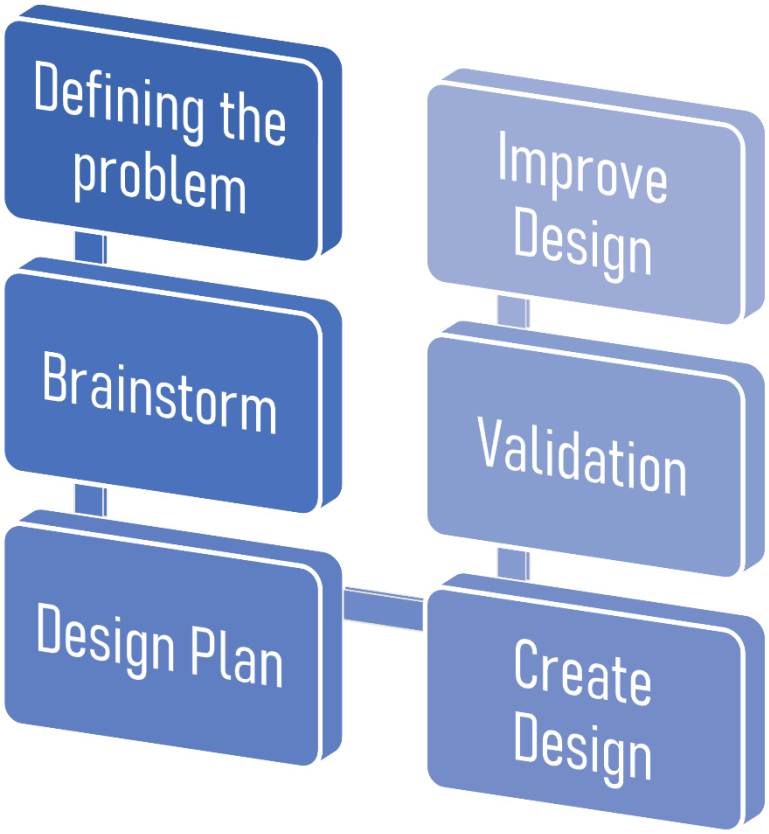

Figure 2.22. Design process

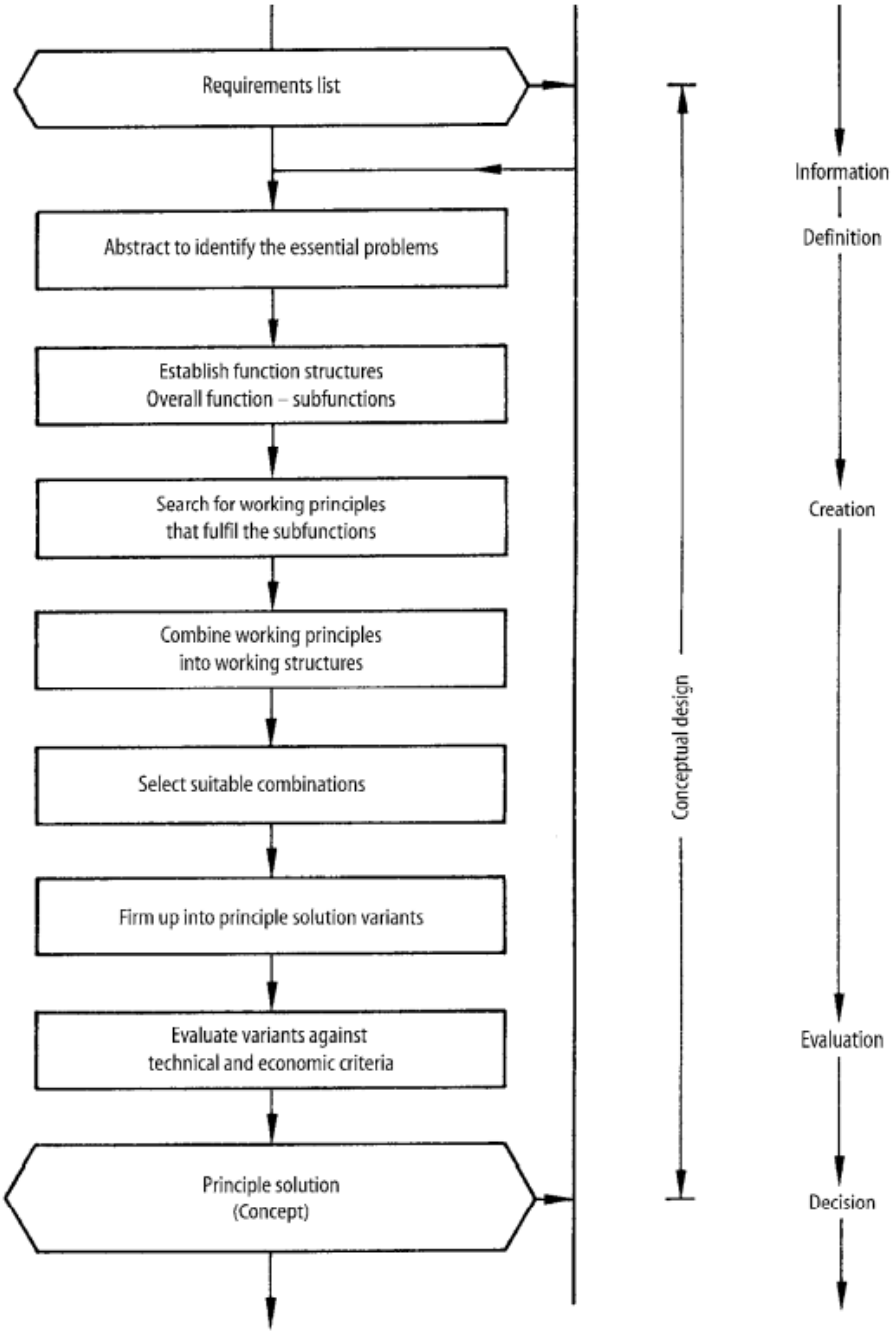

Figure 2.23. Steps of conceptual design (Pahl et al., 2007, p. 160).

Static and topological analysis are the FEA analysis methodologies employed in this thesis. As the name implies, Static analysis calculates the strain, stress, and deformation of an object under load by applying a static load to a specific place. In other words, it mimics the force application that occurs in real-world situations. The research begins by geometrically fixing an entity, preferably at a stationary site in practice. Next, a load is applied to resemble how

force is applied in real life. Finally, the study can be meshed and run once a suitable material has been applied, the geometry has been established, and the load direction and quantity have been defined. Constructing finite elements that are individually analysed to make up a finite element model is known as meshing. The results are later reviewed using plots.

The component is optimized using topology analysis to meet the manufacturing requirements. Similar to static analysis, the goals and restrictions for the design profile can be established. The three main optimization aims are to achieve the best stiffness to weight ratio, minimize mass, and minimize maximum displacement. This thesis focuses on determining how much mass may be eliminated, if any, while still allowing the component to perform as intended. The technique begins similarly to static analysis, with material definition, geometry fixation, and load application. The design goals and limits, such as the proportion of mass eliminated, are established afterwards.

2.5. DFMA Analysis

According to (Tan et al., 2020.), Design for Manufacturing and Assembly (DFMA) is a production philosophy and method that defines manufacturing procedures for various design concepts. The modern manufacturing sectors' constant quest of quality and efficient output has increased the demand for DFMA methodology. As a result, various industries, including automotive, aerospace, and others, are now using DFMA standards in their design and manufacturing processes.

The term DFMA is divided into Design for Manufacturing (DFM) and Design for Assembly (DFA) and the “process integrates the production experience into the product design” as said by (Kuo 2001; Harik and Sahmrani, 2010). This thesis uses DFMA standard in creating the design so that the components of the wheelchair assembly can be manufactured using 3-D printing following DFMA principles. According to Campi (et. al, 2022), following the well-known regulations available from the literature and company

know-how, Design for Manufacturing and Assembly concepts are currently implemented downstream of 3-D modeling.

DFMA philosophy comes in the form of guidelines that are followed to achieve efficient end products. There are no set number of principles, however, there are popular rules that are abundant in every industry. A few of them are listed below:

- Reducing the number of parts for assembly: More number of components manufactured results in higher chances of mishaps during assembly. Hence, a good product which has minimum number of parts cannot be fabricated. (Harik and Sahmrani, 2010)

- Design to aid fabrication: The geometry of the pieces is substantially simpler than for traditional procedures, and any undesirable characteristics are deleted. Also, parts must be designed to fit within the required manufacturing process capabilities. (DB UK, 2017)

- Elimination of cables and adjustments: Cables and attachments cost assembly time significantly. Also, extra adjustments increase the complexity of the manufacturing process. Hence, eliminating them increases the ease in assembly. (Harik and Sahmrani, 2010)

- Minimize use of flexible components: Parts of materials which are uncomfortable to handle such as rubber, cables, gaskets, etc, should be limited to ease part handling and assembly. (DB UK, 2017)

3. CAD design and assembly of wheelchair-power meter

The boundaries that are considered in the design and analysis of the wheelchair-power meter assembly are introduced in this chapter. The design process is next detailed, followed by the parts of the wheelchair and the overall assembly using CAD modelling. The previous approaches to measure power on a paralympic wheelchair discussed in chapter 2 had multiple reasons for not being employed in this current study. Firstly, the use of strain gauges in this thesis was deemed unfeasible due to the nature of the Paralympic wheelchair. Using the strain gauges was to measure the deflection caused by force applied by the athlete on the push rim of the wheelchair. However, the push rim is a curved object and finding a suitable position to place the strain gages while also ensuring the viability of the results was a challenging task. The sample renders of the strain gages placed on the push rim clamps is shown below in figure 3.1.

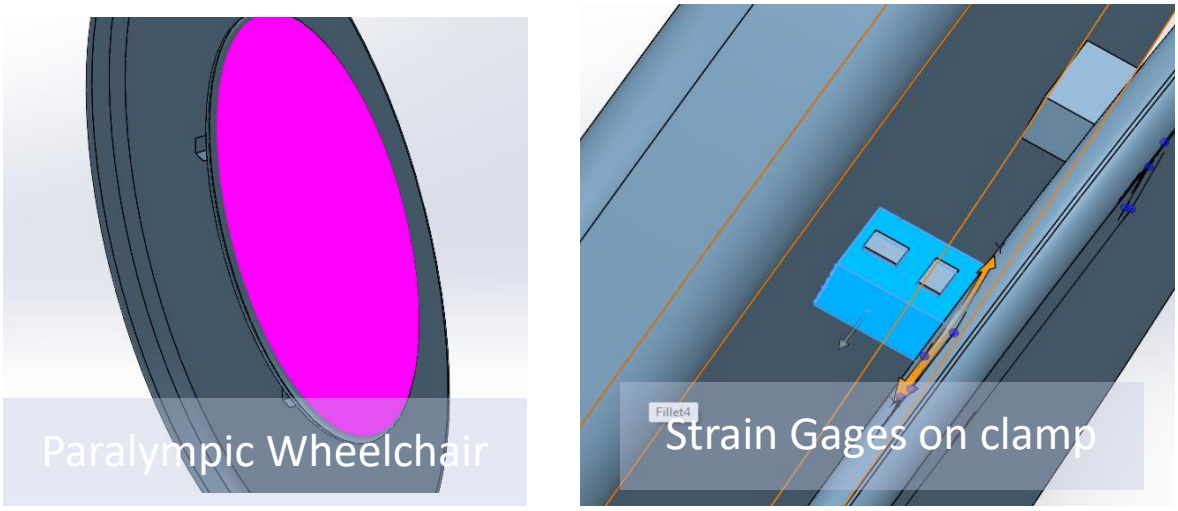

Figure 3.1. Strain Gauges on the push rim

This design concept would be viable only if the athlete's strain could be accurately monitored and measured. The wheelchair clamps must be flat enough to ensure that the gages are placed correctly without external influences for this concept to operate. However, having a flat push rim clamp may reduce the wheelchair's aerodynamic qualities due to drag caused by air

resistance when in motion. Also, this concept makes the entire system more complex while also not guaranteed accurate or semi-accurate results. Hence, this concept was deemed unsuccessful. But the use of strain gauges through a different approach was not omitted because the gauges are capable of measuring power accurately if they are placed optimally while keeping the dynamics of the wheelchair unchanged.

Secondly, the TactileGlove was an interesting concept to explore; however, due to a few crucial considerations, this technology was not used to measure performance in this thesis. To begin with, paralympic racing gloves are rigid three-dimensional constructs with no flexibility. If the sensors are placed inside the glove, they are not sensitive to the pressure exerted on the push rim. If the sensors are put on the outside of the racing glove to monitor pressure, they will have an impact on the glove's ergonomics and riders' performance. Second, each rider's racing gloves are bespoke (or) customized, and the sensors must be positioned in various places for each rider. Even if the accuracy problem has been rectified, this creates a problem throughout product development. Finally, the TactileGlove's most significant drawback is that the glove's most powerful sensor can only measure 70-80 N of force. This is a long cry from the 400-500 N force that an athlete applies to the push rim. The technical parameters of the sensors utilized in the TactileGlove are shown in Figure 2.10, which illustrate the force measurement limitations.

Finally, the concept of using a custom instrumented push rim is an excellent way to assess the paralympic athlete's force application and performance. However, there were various reasons why this method was not used in this thesis that were regarded as shortcomings. To begin, the practicality of this thesis necessitated access to a wind tunnel facility, without which it is difficult to reliably quantify push rim forces due to air drag. Second, the instruments employed in this case study are difficult to comprehend for a public audience and hence, if developed and produced on a big scale, could pose maintenance concerns. Finally, the custom push rim containing all the instruments weighs between 3 and 4 kg. The excess weight could influence the athlete's performance during testing and training, as more weight makes it difficult for the athlete to push the wheelchair forward, and once removed during the race, the rider may experience control challenges due to the wheelchair seeming

lighter. Furthermore, because of the non-uniform weight distribution, putting the custom push rim on only one side of the wheelchair generates a major imbalance in evaluating performance.

3.1. Design Scope and Boundaries

The scope of the design of the wheelchair-power meter assembly is defined in this chapter. The focus is on the assembly of the power meter to one of the rear wheel assemblies of the power meter. A few essential criteria concerning the parts, material properties, design approach, and potential post-processing methods must be identified to ensure there is no aerodynamic shortfall after manufacturing to assure correct results. Further details about the fabrication will be discussed in Chapter 5.

Dimensional requirements, along with the modifications required in the stock wheelchair assembly, were also considered in the design process to attach the power meter to the hub of the wheelchair rear wheel assembly. Table 3.1 gives an overview of the general requirements for the design to be accurate.

Table 3.1. General requirements of design

Weight	Must not exceed 3kg
Aerodynamics	Must ensure there is no excess drag
Modifications	1. Power meter placement must be accurate 2. Power meter should be rigidly attached to the hub 3. Push rim should be modified to allow force transfer to power meter
Dimensions	Must be accurate to ensure perfect assembly

The power meter assembly's size and dimensions were critical factors to examine to ensure that it fits the wheelchair's hub accurately and aids overall functionality. To keep the design

in scope, it was also important to consider some pre-defined dimensions of a few parts that helped the design process and FEA analysis easier.

3.2. Design Process

Design problem, brainstorming, planning, execution, analyzing, and lastly, enhancing the design where the six primary systematic machines develop processes that were utilized to analyze and enhance the wheelchair-power meter.

3.2.1. Design Problem

Incorporating a bicycle power meter into a paralympic wheelchair is a challenging task because there are multiple obstacles to tackle in the design philosophy. The initial study of the wheelchair's dimensions indicated that there is a need for extensive modification to the hub and push rim of the wheelchair due to the dimensions of the power meter. The power meter utilized was a Quark power meter with a 110 mm Bolt circle diameter. The power meter's center must be large enough to accommodate the wheelchair's hub. Furthermore, the power meter must be rigidly attached to the outer surface of the wheel arms to avoid inaccuracy of results.

The second and most important design flaw is that a link between the wheelchair's push rim and the hub is required to effectively transfer force from the rider's hands to the wheelchair, allowing propulsion. The existing link in stock racing wheelchairs does not allow for the inclusion of a power meter, necessitating the modification of the wheelchair's push rim to address the issues. Finally, the third challenge in the design adjustment is maintaining the wheelchairs' aerodynamic efficiency.

3.2.2. Brainstorming

The problems in this study narrowed the scope of the design ideas. The ideation step began with reviewing existing solutions in modern wheelchairs that address the third design issue. During this conceptualization, ideas to avoid aerodynamic losses were adopted and will be examined in detail in Chapter 3.3. This novel technique and design ideas were developed by conducting four approaches, each with its pros and limits, was one of the most difficult elements of investigating numerous solutions for the first two design problems. Before deciding on a final design approach, four options were tested.

3.2.3. Design Plan and Creation

The plan's goal was to find a suitable solution that would combine the positives of each design and incorporate it into the final render. The four options were checked for validity and consistency in changing environments. The first approach was to ensure aerodynamic efficiency, as previously mentioned. The second approach was to test the connection between the hub and the push rim to avoid force losses. Another approach was a combination of aerodynamic efficiency and optimum fitting of the power meter to the wheel's hub.

The issue stemmed from the underlying design difficulty of evaluating several methods for connecting the push rim, power meter, and wheel hub. The solution was tested while considering the structure's primary mechanical criteria, which included strong torque resistance and high yield strength of the materials utilized. After researching existing automobile rims and the reasons for their design, the solution was discovered. Figure 3.2 gives an outlook of an automobile rim from which the answer for the wheelchair push rim was inspired.

Figure 3.2. Ducati Rim (Kienhöffer, 2010).

3.2.4. Testing and Improvement

The final design was tested using Finite Element Analysis and topology analysis to acquire correct findings after it was produced by merging all of the pieces and using DFMA standards for manufacturing the parts using 3-D printing. In addition, Kinstler (2005) developed a load formula that can be used to test the wheelchair design as it resonates with the dynamics of automobiles.

$$M_{bmax} = f * F_{static}(\mu * r_{dyn} + d) \tag{3.1}$$

The maximum bending moment can be estimated using equation 3.1 where M_{bmax} is the maximum bending moment [Nm], f is the frictional factor, F_{static} is the static load [N], r_{dyn} is the dynamic radius of the rim [m]. μ is the co-efficient of friction and d is the diameter in [m].

3.3. CAD Modelling

In the following stages of development, the paper design plans were converted into 3-D models. Then, the single wheel assembly was created from the ground up, considering all of the parameters used in the production of wheelchairs and power meters in real life. The modelling process began with creating a parts list for design and assembly. The parts used and the materials applied to each of them are listed in table 3.2.

Table 3.2. List of parts for wheelchair-power meter design

Parts	**Quantity**	**Material**	**Dimensions and Properties**
Nuts	5x	Stainless Steel	Diameter: 11.55mm
Bolts	5x	Stainless Steel	Diameter: 6mm
Power meter	1x	Plastic	Bolt Circle Diameter: 110mm
Wheelchair push rim	1x	AL 6061-T6	Diameter: 14 inches
Wheel	1x	AL 6061-T6	Diameter: 24.49 inches

The first component to be modeled was the wheelchair. The specifications of the wheelchair wheel and push rim came from various sources, including a literature review, reading manufacturers' catalogs, talking to paralympic coaches, and looking at real-world racing wheelchairs. The diameter of the wheel varies between 23 and 25 inches, depending on the preferences of the athletes. Because it is an average of all sizes of wheels utilized in this design research, the diameter was set at 24.5 inches. In addition, the dimensions gathered from the above sources were used to model the push rim. The push rim's diameter ranges from 13 to 15 inches, with 14 inches used in this experiment.

Most current wheelchairs are constructed from aluminum, steel, or titanium. The wheel and push rim frames were made of aluminum 6061-T6, a common form of aluminum used in manual and sports wheelchairs. It is the most significant grade of aluminum accessible for

these applications, has a higher strength-to-weight ratio than mild steel, and is corrosion-resistant. The mechanical properties of Al 6061-T6 are presented in Table 3.3.

Table 3.3. Properties of Al 6061-T6

Property	**Value**	**Units**
Elasitc Modulus	6.900000067e10	N/m^2
Poisson's Ratio	0.33	-
Yield Strength	275000000.9	N/m^2
Tensile Strength	310000002.1	N/m^2
Mass Density	2700	Kg/m^3
Shear Modulus	2.600000013e10	N/m^2

The hub of the wheelchair is shown in figure 3.3 where the power meter is attached to the wheelchair and power meter.

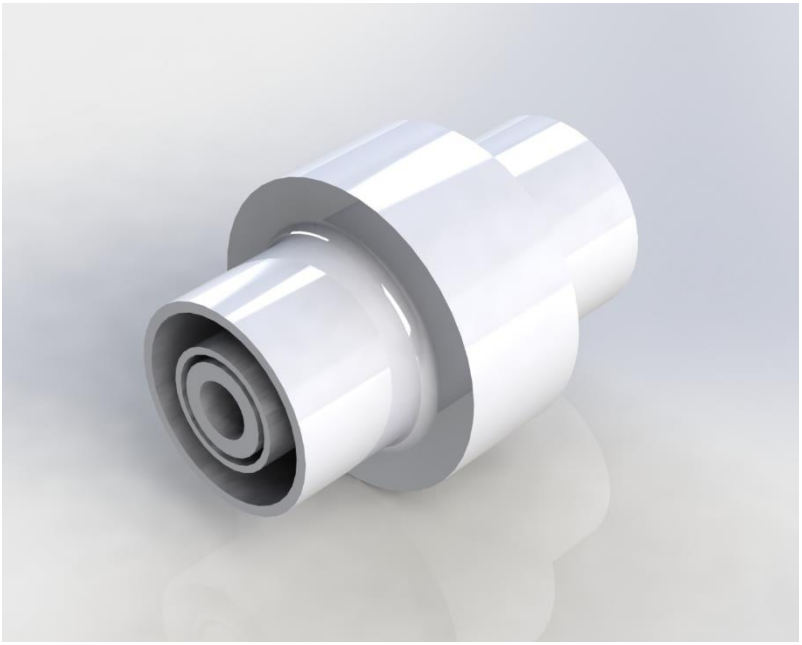

Figure 3.3. CAD render of Wheelchair Hub

The power meter was next to be modelled. According to the manufacturer's literature, the Bolt Circle Diameter of the quarq dzero dub power meter is 110 mm. To comprehend the specifics of the design, hand sketches of the power meter were created. The model was then built on Solidworks 2020, with the essential components like the hub and bolt holes throughout its circle being as realistic as feasible. In addition, the strain gauges are housed on a flat protrusion along the perimeter of the power meter, which is another essential feature. As a result, it was critical to position the power meter flat above the wheelchair's hub. Two adjustments to the existing wheelchair were required to accomplish this.

Before making any alterations, the racing wheelchair's wheel must be covered with a carbon fiber plate of the same diameter as the wheel, as described in Chapter 3.1. Therefore, the initial change was to create a flat circular plate and place it over the wheelchair's hub and the carbon fiber plate. The power meter will be able to rest precisely flat above the center due to this. Figure 3.4 shows the CAD model of the power meter.

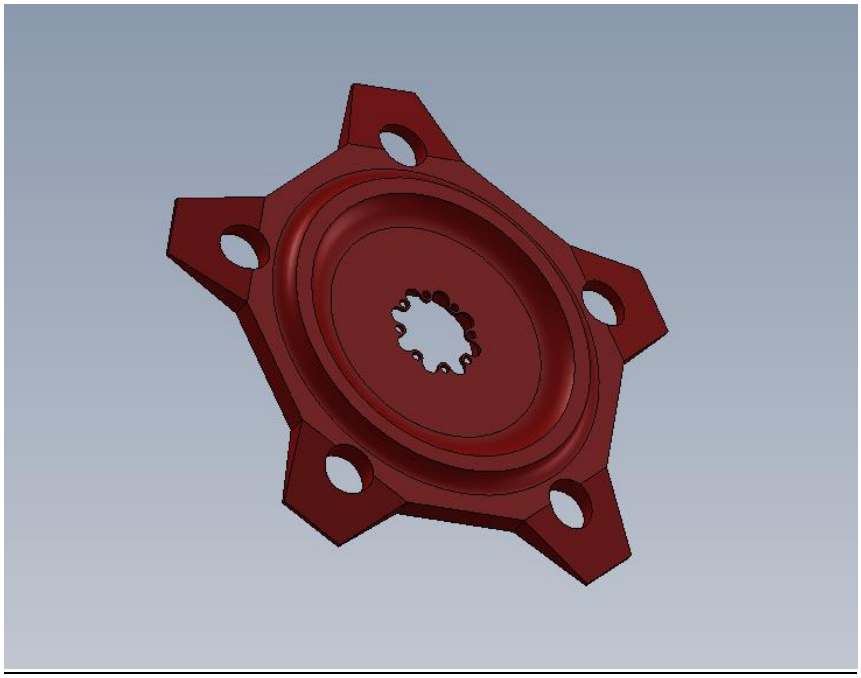

Figure 3.4. 3-D model of Quarq Dzero Dub power meter

The power meter is built of solid polymers of unknown grade. However, the longevity or performance of the power meter in the wheelchair assembly is unaffected by the plastic quality. Table 3.4 shows the mechanical properties of available plastics.

Table 3.4. Properties of Plastics

Property	**Value**	**Units**
Elastic Modulus	6000000	N/m^2
Poisson's Ratio	0.47	-
Shear Modulus	2000000	N/m^2
Tensile Strength	13000000	N/m^2
Mass Density	1290	Kg/m^3

Five holes must be bored in the carbon fiber plate to secure the power meter's ends (bolt holes) to the wheelchair. Next, bolts and nuts must be used to secure the power meter rigidly to the wheelchair. There are five nuts and bolts used to fix the power meter to the wheelchair, and they were also modeled on CAD with the necessary proportions based on the specifications of the power meter. The bolts are of 6mm diameter with external threads along the length. The nuts were designed to meet the bolts' size, with internal lines to fit the bolts' threads.

Because stainless steel is widely used in the industry, it was chosen for the nuts and bolts. The usage of these materials also aligns with the thesis' secondary goal of simplifying the design so that it may be reverse engineered without much knowledge. The material properties of this grade of stainless steel are presented in table 3.5.

Table 3.5. Properties of stainless steel

Property	Value	Units
Elastic Modulus	1.929999974e11	N/m^2
Poisson's Ratio	0.27	-
Yield Strength	172368932.3	N/m^2
Tensile Strength	580000000.8	N/m^2
Mass Density	8000.000133	Kg/m^3

The final assembly was modelled using Design for Manufacturing and Assembly (DFMA) principles after combining all parts. The DFMA principles that were followed are given below:

- **Reduce number of parts to a minimum**: The wheelchair power meter was created with only the pieces required for the component to function. The only additional components required for functioning are the adjustments made to the push rim assembly and the aluminum plate for housing the power meter.

- **Standardization**: Almost all components of the wheelchair-power meter have standard dimensions and materials to ensure easy access to the essential components in the event of failure or replacement. The nuts and bolts are composed of stainless steel and come in a variety of sizes. The power meter and wheelchair are both conventional parts with predetermined dimensions. The only custom adjustments to the designs are the connections between the push rim and the hub and power meter, which can also be made out of aluminum, which is a readily available material.

- **Ease of assembly and handling**: The power meter is fastened to the wheelchair assembly with simple nuts and bolts. It is easy to handle and transport because the entire assembly weighs less than 2-3 kg.

Due to the design's complexity, a few DFMA considerations could not be applied. It's still unclear which manufacturing method would be used to fabricate the components, and design complexity may play a role in determining if it'll be compatible with a variety of procedures. A schematic diagram of the wheelchair assembly is shown in figure 3.5.

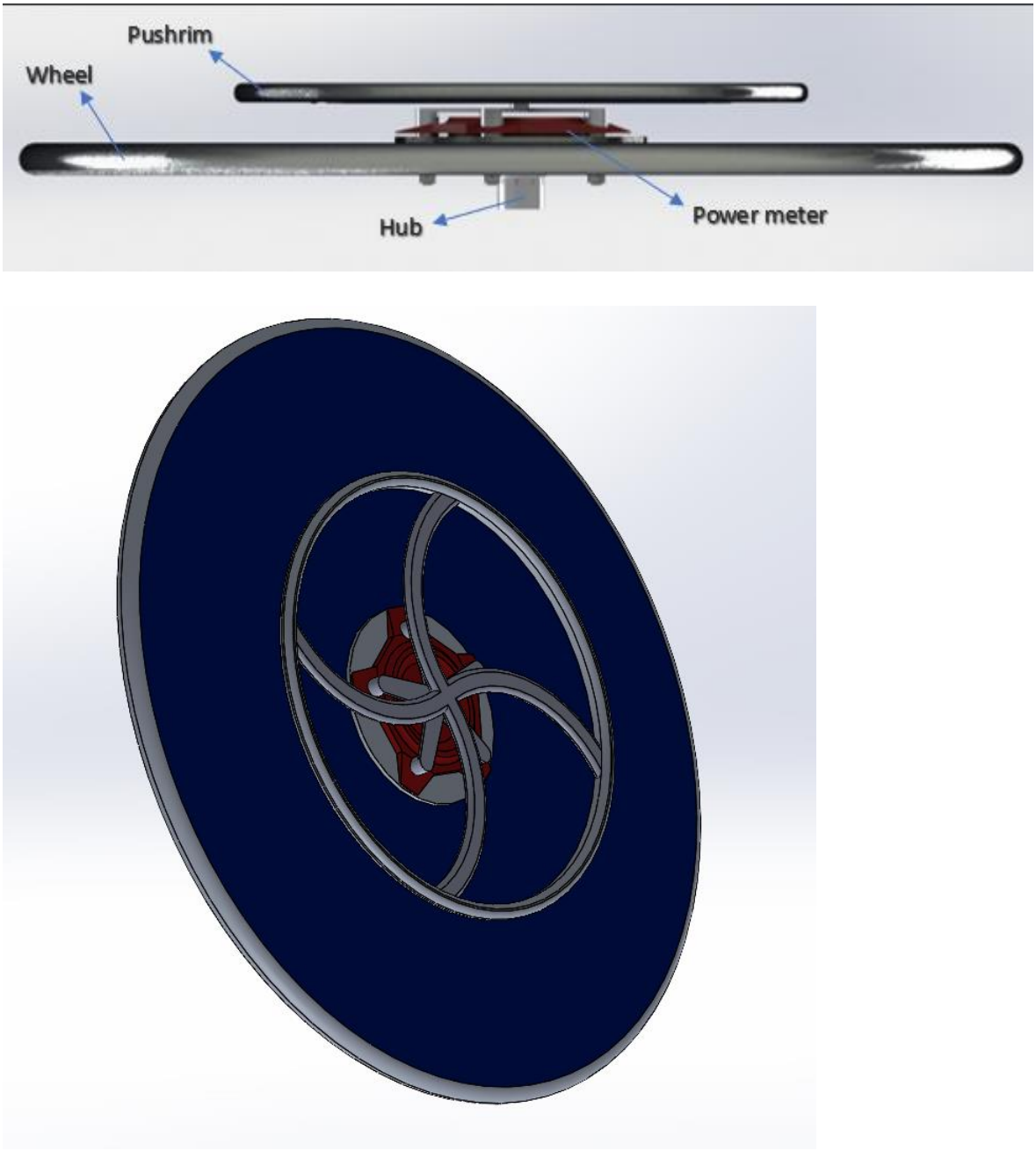

Figure 3.5. a) Schematic 3-D Model of wheelchair assembly b) Isometric model of wheelchair assembly

The extra attachment from the center of the push rim to the ends of the power meter is shown in figure 3.6. This link guarantees that force is transferred consistently from the athlete's hands to the wheelchair. The torque input can then be recorded and converted into power in Watts by the power meter.

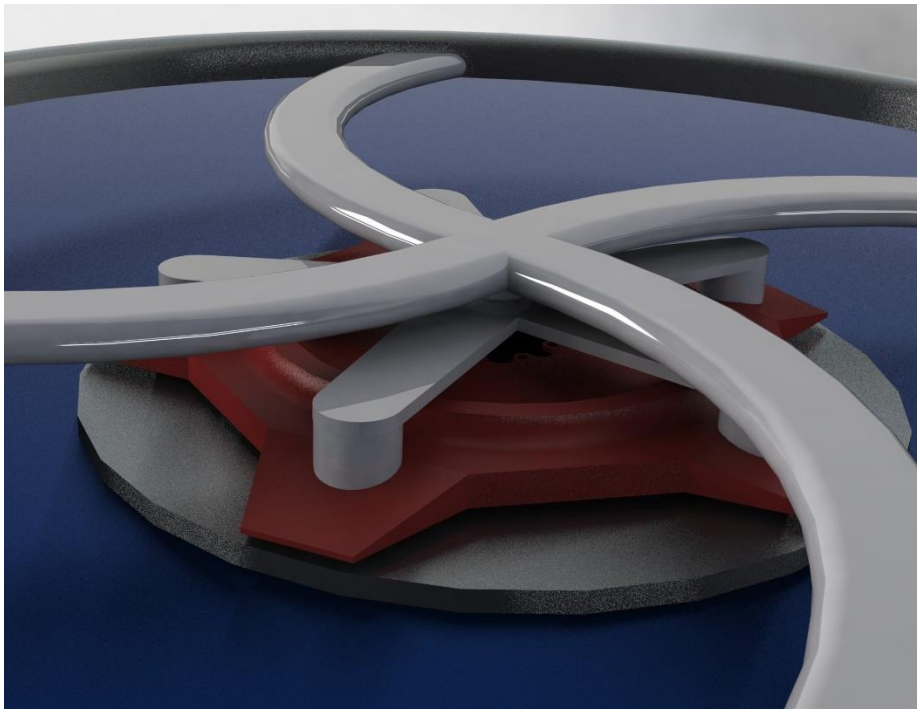

Figure 3.6. CAD Renders of the push rim attachment to the bolt holes of power meter

In the appendix portion of the report, an alternate design concept is offered, and general ideas linked to Systematic Machine Design (SMD) guidelines used to conceptualize this method are presented.

4. Results and Discussion

This section highlights the FEA results for the power meter-wheelchair assembly. The point load highlights the static displacement. The strain caused by force applied to the push rim was also measured. The static nodal stress (also known as von Mises stress) was also evaluated, and the results of all tests are presented in this chapter. The findings will also be examined to understand how well they address the research problem.

4.1. FEA analysis

This section displays the wheelchair assembly's Finite Element Analysis results. The FEA study was a static analysis study that began with applying the proper material to all components. The wheel and power meter were left out of this study since meshing the intricate portions of these components needs a lot of GPU power and can lead to meshing failures if the geometry is too complex. Figure 4.1 shows the CAD render of the push rim modification used for analysis.

Figure 4.1. Push rim modification

The next stage was to fix a geometry at the hub and apply a force of 500 N to the push rim's diameter. The meshing intensity was set to an average of entirely fine and completely coarse meshing. Figure 4.2 shows the geometry fixation at the hub attachment of the push rim assembly.

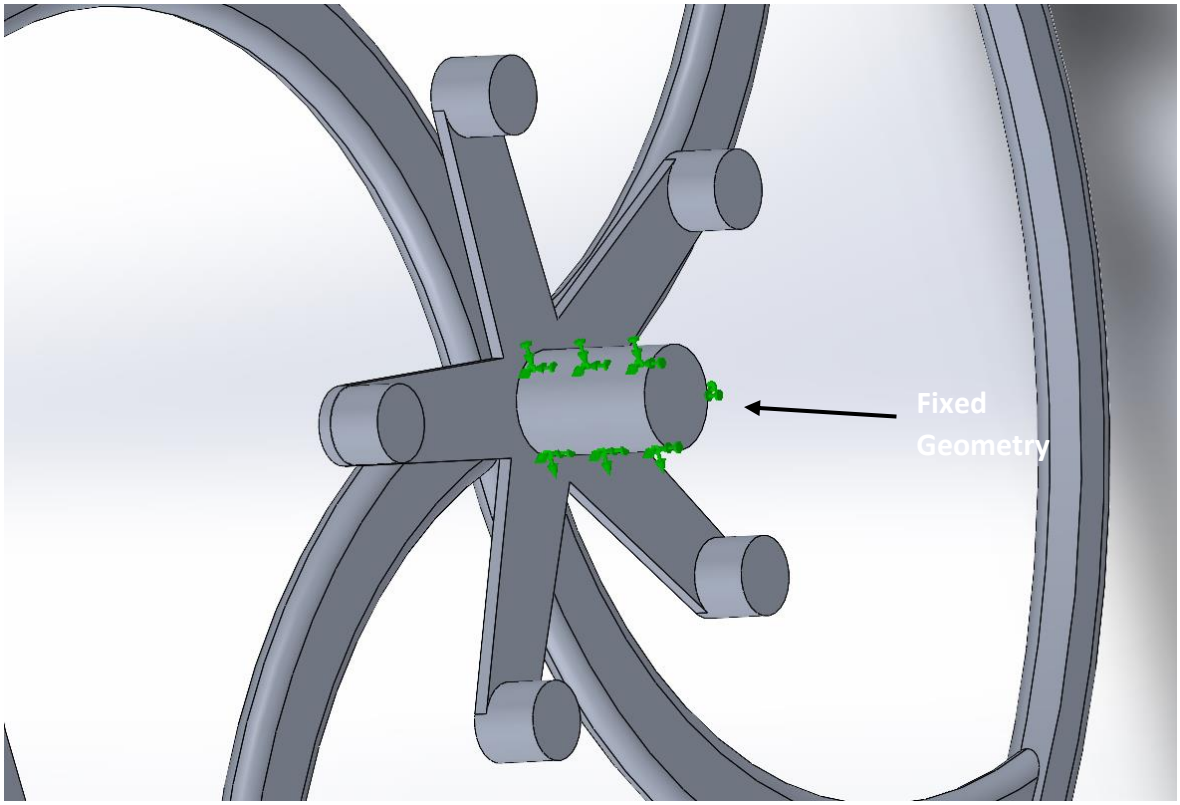

Figure 4.2. Fixing geometry at the hub of push rim assembly

Figure 4.3 depicts the application of force along the push rim, simulating real-world motion of the push rim after the athlete has applied force.

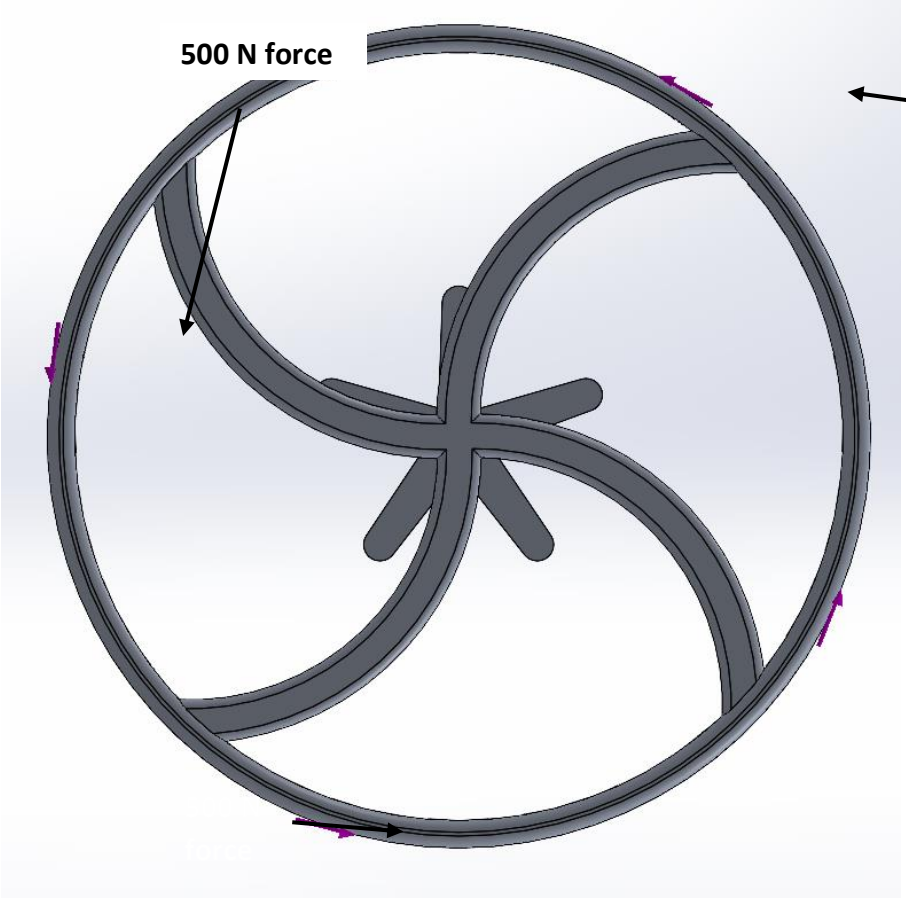

Figure 4.3. Force application on push rim

The final result of the static analysis is shown in figure 4.4 and the individual plots will be shown further.

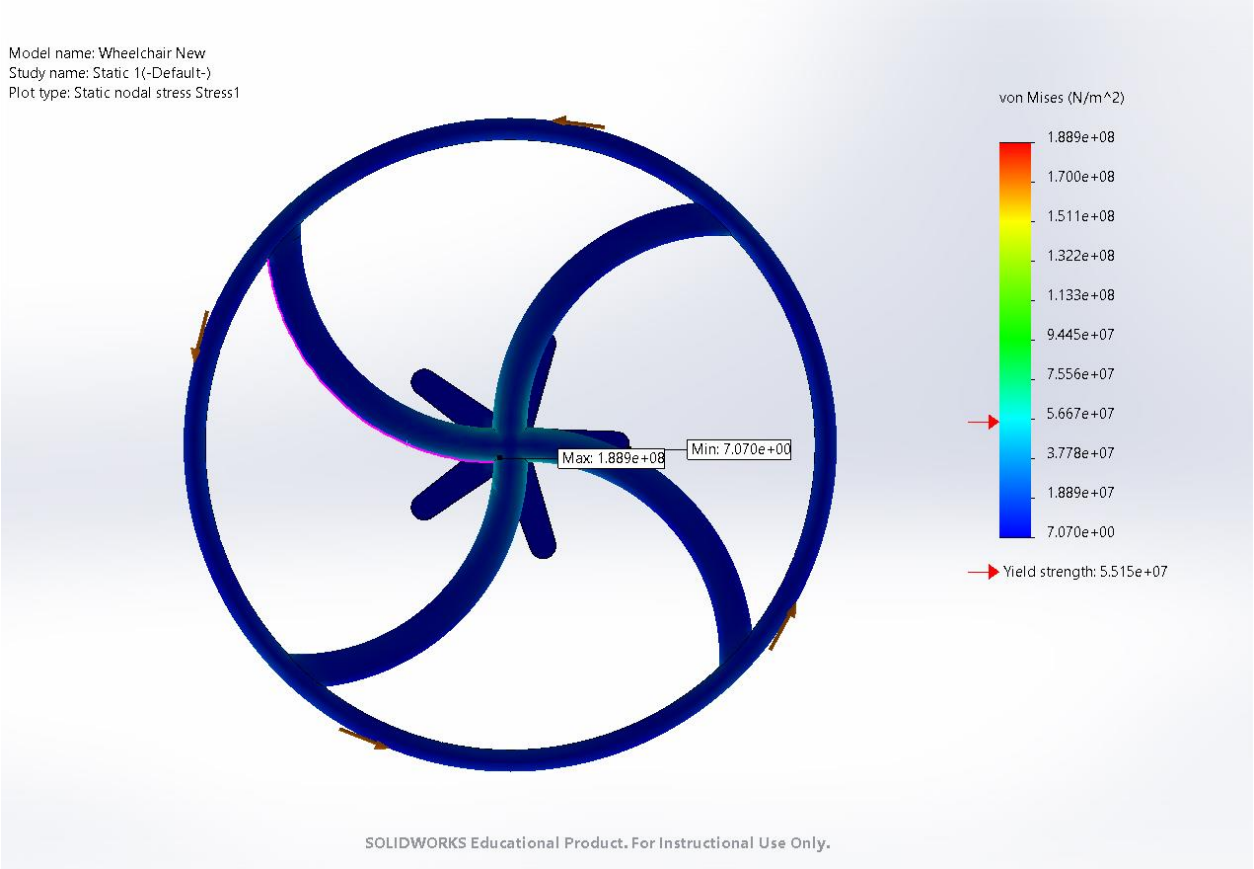

Figure 4.4: Push rim after static analysis

In Figure 4.5, the von Mises stress on the push rim is depicted. The push rim is more affected than the hub by the pressure after 500 N of force, which is more than the usual. This also means that the arms connecting the hub and the rim are strong enough to keep the structure intact under a realistic load. After static analysis, the yield strength of the resulting push rim is 5.515e7 MPa. The highest stress applied at the hub is 1.889e8 MPa, whereas the lowest pressure applied at the push rim modified component attached to the power meter is 7.07 MPa.

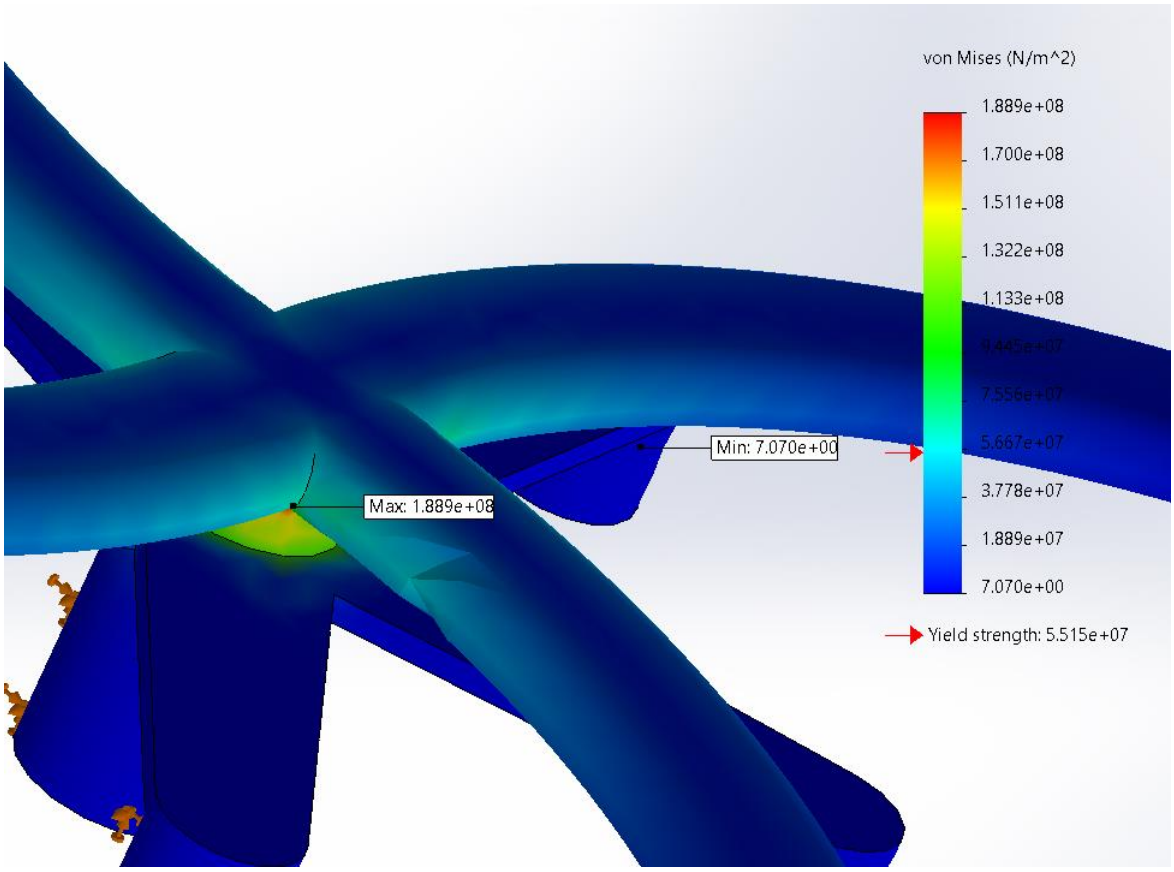

Figure 4.5: von Mises stress on push rim assembly

The strain induced in the push rim assembly is shown in the figure 4.6. The maximum strain induced is 2291e9 mm at the hub.

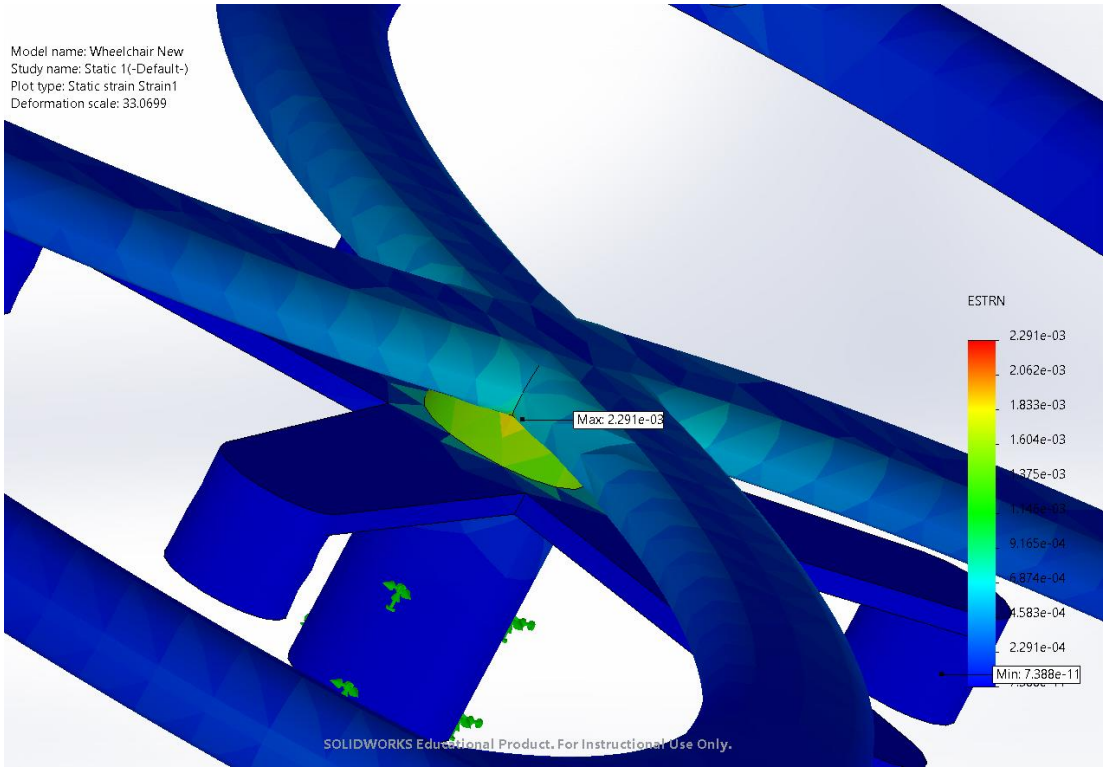

Figure 4.6: Strain induced on push rim

With a maximum distortion of 1.083mm, the displacement was recorded along the whole push rim in figure 4.7. The distortion starts at the push rim and proceeds through the spolks towards the hub. However, the hub is not affected, and the reasons will be mentioned in chapter 4.2

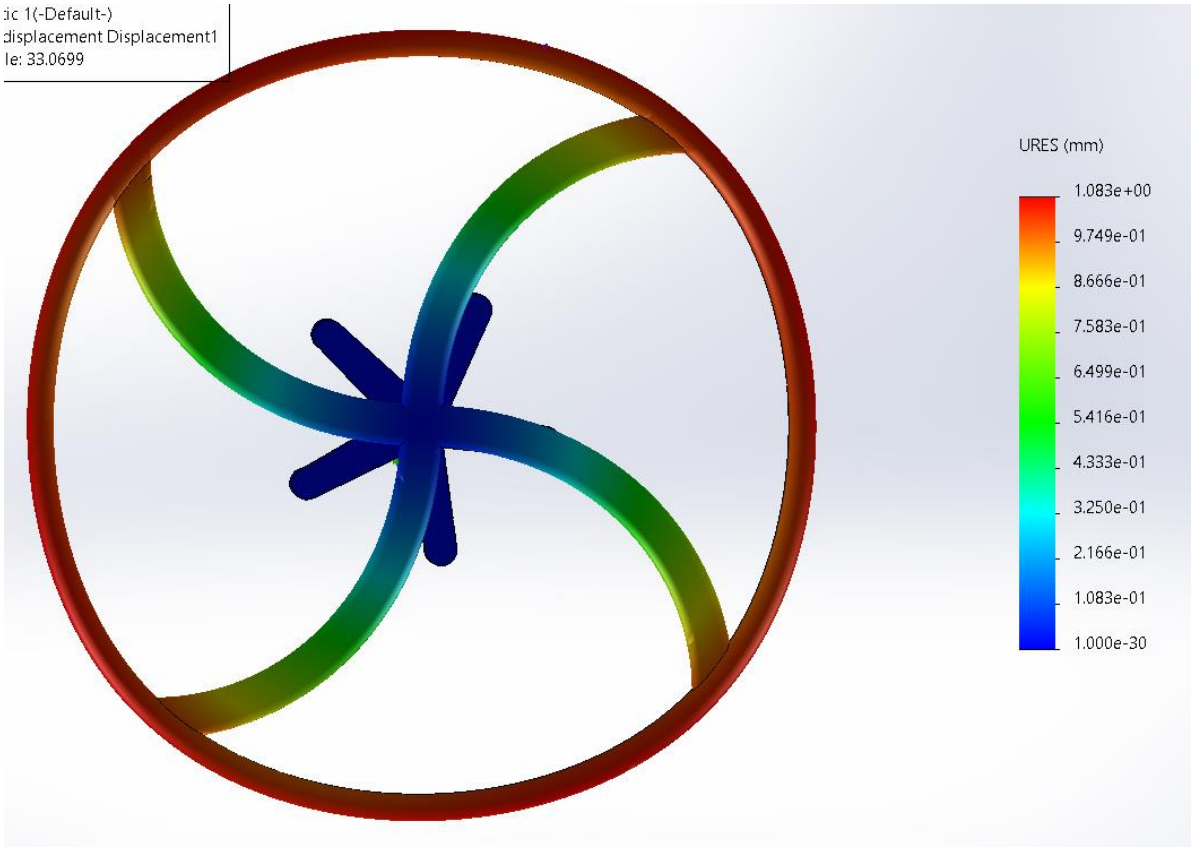

Figure 4.7: Deformation on push rim

The final research was a topology analysis. The system removes any unwanted mass by running many iterations of surface analysis to examine the structure's weak areas and minimize the overall weight. As indicated in the design challenge, it is vital to reduce weight as much as possible. The simulation took over 20 minutes to complete 30 iterations in the topology research. Figure 4.8 depicts the results of the topological study, which will be detailed in Chapter 4.2. The calculated element mass before the analysis was 0.67817 kg, and the mass after the study was 0.55989 kg.

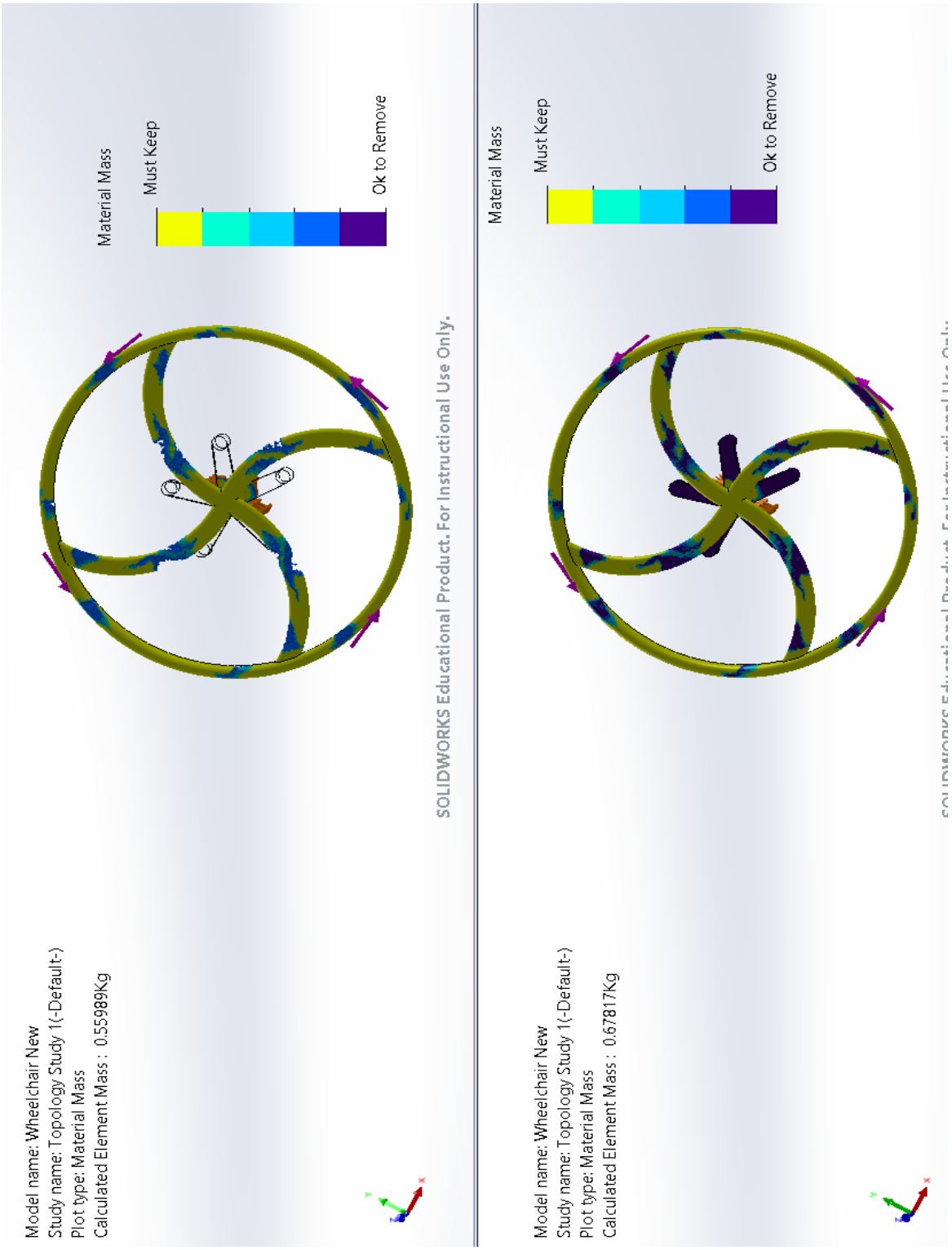

Figure 4.8: Topology analysis on push rim assembly

4.2. Discussion

The built CAD model is promising, but if the DFMA limits were less rigorous, further testing might be possible. Once fully designed, the wheelchair assembly will demonstrate the true implications of the power meter combo. However, when compared to the initial hypotheses, the findings of this study are optimum. The results of this study's literature were crucial in identifying issues that this thesis tries to avoid compared to previous methodologies. It was also helpful in developing the current approach by providing information on existing power measurement technology. The wheelchair's rear wheel assembly was designed and joined with the quarq power meter without too many issues, however, with considerable alterations. The use of Systematic Machine Design (SMD) recommendations was limited due to the limited scope of this study. Still, they were employed effectively by nudging the concept in the right direction.

The Finite Element Analysis (FEA) results indicate how to proceed with design and fabrication development. The static analysis of the wheelchair assembly shows that the push rim deforms slightly under 500 N force application. In a real-world scenario, however, the deformation will be minimal because the entire wheelchair assembly will assist in evenly distributing stresses and weight distribution on both sides of the wheelchair. The deformation begins around the circle of the push rim and ends just before it reaches the hub. The force travels to the hub through the four spolks of the push rim, which is vital to remember. This result is perfect since the power meter will capture the forces traveling to the hub during the athlete's many propulsion cycles. The maximum stress created at small parts of the hub exceeds the material's yield strength. This was to be expected, given that this was the power meter's attachment point and the modified push rim parts. The aluminium hub's results need not be accurate as of the push rim, and its arms are the focal point. It won't hinder the wheelchair's overall performance because the entire model will assist balance the weight, resulting in a higher strength-to-weight ratio.

The strain measured at the hub is far too tiny to create any deformation. It's natural to assume that the power meter has strain gauges that will record these strains; however, the power

meter can only record the torque applied by the athlete to the push rim, and it calculates power using the force from the push rim rather than the hub. Therefore, the topological analysis determined where the assembly mass might be eliminated without compromising durability. The results showed that removing a few bits of material from the arms of the push rim reduced the element's mass by 118 grams. Although weight loss is generally advantageous, it is less crucial in this case than predicted. The initial weight was 600 grams, which was already perfect for the overall goal. Furthermore, material loss would put the durability in danger due to long-term part fatigue from repetitive actions.

The thesis left out a key factor: assessing the cost of the power meter device and the cost of production and assembly of all elements. Although the cost of the power meter is known and is relatively affordable, it is difficult to estimate the cost of fabricating the complicated parts because it is unclear what manufacturing procedures can be employed.

5. Conclusions

The goal of this research was to establish a simple way to measure a paralympic athlete's performance where coaches and athletes do not have to depend on complicated instrumented objects to measure how well they are doing. This motivation led to the development of this thesis where a cycling power meter was integrated onto a Paralympic wheelchair which was the primary objective. This thesis also aims to answer research questions that were established at the beginning of the research. They are:

1. How can the performance be quantified and improved?
2. Which is the best method to measure power in a wheelchair?
3. How do we incorporate bicycle power measurement technology into racing wheelchairs?
4. How can the design corelate with real life application?

This thesis accurately solves all research questions. As the literature review in this thesis shows, a paralympic athlete's performance can be measured in various ways. However, the easiest way to quantify quantitative performance is to focus on one or more essential characteristics like velocity, cadence, power, torque, etc. This thesis examines using a Quarq Dzero Dub power meter to record an athlete's torque input in wheel-based sports. Calculating the power input and time taken to finish a certain distance and making modifications based on those figures can improve performance.

Because there are various ways to measure power accurately, the optimum method to measure power is a highly subjective idea. This thesis demonstrates several approaches, including creating a specially instrumented push rim, a suitable method for measuring power correctly. This technology, however, was not used in this thesis because it concentrated on a more straightforward, easier-to-maintain way of measuring power by integrating a power meter into a wheelchair. The power meter is a device that directly measures power. As a result, there is no objectively optimum method for measuring power because multiple

methods are utilized depending on the user's preferences. For example, some customers want a measurement system that is simple to use, while others require a thorough approach where precision is critical.

The ability of a power meter to capture power input by the rider at the crank (or) hub of the bicycle is critical to its use in a bike. The bicycle's crank arms transmit the torque. As a result, it was imperative to determine the appropriate placement, type of power meter, and how the torque transfer from the point of application to the power meter could be replicated. The hub of the wheelchair, like the hub of a bicycle, is a unique place to measure power. The wheelchair's push rim assembly has been modified to ensure that the power provided to the rim travels through the arms of the push rim and to the hub. In addition, the power meter is anchored at all five ends to ensure that the strain gauges accurately register the torque. As a result, this thesis accurately solves the question of how to integrate a bicycle power meter into a Paralympic wheelchair.

Manufacturability was considered during the study of the power meter integration. The parts and materials utilized are widely available and straightforward to produce, whether through traditional manufacturing or additive manufacturing. Furthermore, with the support of a paralympic athlete, the designs can be developed, built, and tested in the future. As a result, they are intended for future manufacture and testing to improve athlete performance.

The thesis has met its primary goal and, to the best of the author's knowledge, also answers the research questions. However, there are a few areas where progress and improvement are still possible. For example, the use of Design for Manufacturing and Assembly (DFMA) principles to optimize designs is one of the themes that could have been discussed more thoroughly. The objects designed in this thesis can be easily fabricated using DFMA, and the precise ideas followed by each part could have been highlighted thoroughly.

One of the study's critical flaws is that the power meter utilized is quite specific. There is only one sort of power meter in the designs that can be used. i.e., the Quarq Dzero Dub

power meter. Although this type of power meter is abundantly available and is manufactured by multiple companies, it's evident that the wheelchair assembly is centered on the power meter's use; any changes to the shape of the power meter will significantly impact wheelchair designs. With future iterations, this constraint can be investigated further and improved.

The manufacturing procedure used to produce the designs was not extensively discussed. This is because more research is required to fully comprehend the manufacturability of each part before selecting a fabrication method. Furthermore, the manufacturing process impacts the overall development cost and may necessitate changes following the systematic design process (SMD).

References

Cooper, R.A., 1990. Wheelchair racing sports science: a review. J Rehabil Res Dev, 27(3), pp. 295-312.

Tutak, P., 2014. Application of strain gauges in measurements of strain distribution in complex objects. Journal of Applied Computer Science Methods, p. 6.

Kester, W., 2005. Strain, Force, Pressure and Flow Measurements. In Op Amp Applications Handbook (pp. 247-256).

IQS Directory. Strain Gauge. [On IQS Directory's website]. [Referred on 26.03.2022]. Available: https://www.iqsdirectory.com/articles/load-cell/strain-gauge.html

Hoffmann, K., 2012. An introduction to stress analysis and transducer design using strain gauges, p. 127.

Forte, P., Barbosa, T.M. and Marinho, D.A., 2015. Technologic appliance and performance concerns in wheelchair racing–helping Paralympic athletes to excel. New perspectives in fluid dynamics, pp.101-121.

Barbosa, T.M. and Coelho, E., 2017. Monitoring the biomechanics of a wheelchair sprinter racing the 100 m final at the 2016 Paralympic Games. European Journal of Physics, 38(4), p.10.

Forte, P., Marinho, D.A., Morais, J.E., Morouço, P.G. and Barbosa, T.M., 2018. Estimation of mechanical power and energy cost in elite wheelchair racing by analytical procedures and numerical simulations. Computer Methods in Biomechanics and Biomedical Engineering, 21(10), pp.585-592.

Covill, D., King, R., Townsend, J., Brickley, G. and Drouet, J.M., 2020. Development of Customised Wheelchair Racing Gloves Using Digital Fabrication Techniques. In Multidisciplinary Digital Publishing Institute Proceedings 49(1), p. 44.

Rice, I., Dysterheft, J., Bleakney, A.W. and Cooper, R.A., 2016. The influence of glove type on simulated wheelchair racing propulsion: A pilot study. International Journal of Sports Medicine, 37(01), pp.30-35.

Pressure Profile. Tactile Glove. [On Pressure Profile's website]. [Referred on 27.03.2022]. Available: https://pressureprofile.com/body-pressure-mapping/tactile-glove

Designing Buildings UK. Design for Manufacture and Assembly. [On Designing Buildings' website]. [Referred on 10.05.2022]. Available: https://www.designingbuildings.co.uk/wiki/Design_for_Manufacture_and_Assembly_(DfMA)

DesignMeasurement of push-rim forces during racing wheelchair propulsion using a novel attachable force sensor system. Proceedings of the Institution of Mechanical Engineers, Part P: Journal of Sports Engineering and Technology, pp. 1-10.

Chénier, F., Pelland-Leblanc, J.P., Parrinello, A., Marquis, E. and Rancourt, D., 2021. A high sample rate, wireless instrumented wheel for measuring 3D pushrim kinetics of a racing wheelchair. Medical Engineering & Physics, 87, pp.30-37.

Limroongreungrat, W., Wang, Y.T., Chang, L.S., Geil, M.D. and Johnson, J.T., 2009. An instrumented wheel system for measuring 3-D pushrim kinetics during racing wheelchair propulsion. Research in Sports Medicine, 17(3), pp.182-194.

Pelland-Leblanc, JP, Lépine, J., Champoux, Y. and Drouet, JM, 2014. Using power as a metric to quantify vibration transmitted to the cyclist. Procedia Engineering , 72 , pp.392-397.

Mcainsh, Richard. (2014). Design and Engineering of an Accurate Bicycle Power Meter. [Conference Paper]. [Referred on 25.03.2022] Available: https://www.researchgate.net/publication/303517617_Design_and_Engineering_of_an_Accurate_Bicycle_Power_Meter

Fuglsang, T., 2015, Development and evaluation of a novel power meter device in cycling: a proof of concept study. Gr. 1047 Sports Technology – AAU. [PDF Document]. [Referred on 18.10.2021]. Available: https://projekter.aau.dk/projekter/files/213429322/grp1047bedoemmelse2015.pdf

Bouillod, A., Soto-Romero, G., Grappe, F., Bertucci, W., Brunet, E. and Cassirame, J., 2022. Caveats and Recommendations to Assess the Validity and Reliability of Cycling Power Meters: A Systematic Scoping Review. Sensors, 22(1), p.386.

Isacco, L., Ritter, O., Tordi, N., Laroche, D., Degano, B., Bouhaddi, M., Rakobowchuk, M. and Mourot, L., 2016. Similar substrate oxidation rates in concentric and eccentric cycling matched for aerobic power output. Applied Physiology, Nutrition, and Metabolism, 41(11), pp.1204-1207.

Majerczak, J., Grandys, M., Duda, K., Zakrzewska, A., Balcerczyk, A., Kolodziejski, L., Szymoniak-Chochol, D., Smolenski, R.T., Bartosz, G., Chlopicki, S. and Zoladz, J.A., 2017. Moderate-intensity endurance training improves endothelial glycocalyx layer integrity in healthy young men. Experimental physiology, 102(1), pp.70-85.

Ménétrier, A., Pinot, J., Mourot, L., Grappe, F., Bouhaddi, M., Regnard, J. and Tordi, N., 2013. Effects of recovery using contrast water therapy or compression stockings on subsequent 5-min cycling performance. Journal of Science and Cycling, 2(2), pp.49-56.

Bouillod, A., Pinot, J., Soto-Romero, G., Bertucci, W. and Grappe, F., 2017. Validity, sensitivity, reproducibility, and robustness of the PowerTap, Stages, and Garmin Vector power meters in comparison with the SRM device. International Journal of Sports Physiology and Performance, 12(8), pp.1023-1030.

Miller, M.C., Macdermid, P.W., Fink, P.W. and Stannard, S.R., 2015. Agreement between Powertap, Quarq and Stages power meters for cross-country mountain biking. Sports Technology, 8(1-2), pp.44-50.

Daniels, D., 2017. Sensor Technologies for Determining Cyclist Power Output: A Comparison of Smartphone, Opposing Force and Strain Gauge Power Measurement Technologies Using Spatial Analysis (Doctoral dissertation, University of Southern California), p. 10.

Mehmood, N.Q. and Culmone, R., 2015, March. An ANT+ protocol based health care system. In 2015 IEEE 29th International Conference on Advanced Information Networking and Applications Workshops (pp. 193-198). IEEE.

Vanlandewijck, Y., Theisen, D. and Daly, D., 2001. Wheelchair propulsion biomechanics. Sports medicine, 31(5), pp.339-367.

Higgs, C., 1986. Propulsion of racing wheelchairs. In Sport and disabled athletes. 1984 Olympic Scientific Congress Proceedings, Vol. 9, pp. 165-172.

Thacker, J. and Foraiati, K., 1991. Ride comfort. Wheelchair mobility: Improved wheelchair and seating design, summary of activities February, pp. 27-33.

Van der Woude, L.H.V., Geurts, C., Winkelman, H. and Veeger, H.E.J., 2003. Measurement of wheelchair rolling resistance with a handle bar push technique. Journal of medical engineering & technology, 27(6), pp.249-258.

Lin, J.T., Huang, M. and Sprigle, S., 2015. Evaluation of wheelchair resistive forces during straight and turning trajectories across different wheelchair configurations using free-wheeling coast-down test. Journal of Rehabilitation Research & Development, 52(7).

Asato, K.T., Cooper, R.A., Robertson, R.N. and Ster, J.F., 1993. SMART/sup Wheels: development and testing of a system for measuring manual wheelchair propulsion dynamics. IEEE Transactions on Biomedical Engineering, 40(12), pp.1320-1324.

Finley, M.A., Rasch, E.K., Keyser, R.E. and Rodgers, M.M., 2004. The biomechanics of wheelchair propulsion in individuals with and without upper-limb impairment. Journal of rehabilitation research & development, p. 41.

Wu, H., Berglund, L. J., Su, F., Yu, B., Westreich, A., Kim, K., and An, K. (August 1, 1998). "An Instrumented Wheel for Kinetic Analysis of Wheelchair Propulsion." ASME. J Biomech Eng. August 1998; 120(4): 533–535

Robertson, R.N., Boninger, M.L., Cooper, R.A. and Shimada, S.D., 1996. Pushrim forces and joint kinetics during wheelchair propulsion. Archives of physical medicine and rehabilitation, 77(9), pp.856-864.

Caspall, J.J., Seligsohn, E., Dao, P.V. and Sprigle, S., 2013. Changes in inertia and effect on turning effort across different wheelchair configurations. Journal of Rehabilitation Research & Development, 50(10).

Brubaker, C.E., 1986. Wheelchair prescription: an analysis of factors that affect mobility and performance. J Rehabil Res Dev, 23(4), pp.19-26.

Fuss, F.K., 2009. Influence of mass on the speed of wheelchair racing. Sports Engineering, 12(1), pp.41-53.

Coutts, K.D., 1991. Dynamic characteristics of a sport wheelchair. J Rehabil Res Dev, 28(3), pp.45-50.

Tan, T., Lu, W., Tan, G., Xue, F., Chen, K., Xu, J., Wang, J. and Gao, S., 2020. Construction-oriented design for manufacture and assembly guidelines. Journal of Construction Engineering and Management, 146(8), p.1.

Kuo, T.C., Huang, S.H. and Zhang, H.C., 2001. Design for manufacture and design for 'X': concepts, applications, and perspectives. Computers & industrial engineering, 41(3), pp.241-260.

Harik, R.F. and Sahmrani, N., 2010. DFMA+, a quantitative DFMA methodology. Computer-Aided Design and Applications, 7(5), pp.701-709.

Beitz, W., Pahl, G. and Grote, K., 1996. Engineering design: a systematic approach. Mrs Bulletin, 71

Appendix 1: Tables containing comparisons between different power meters (Bouillod et. al 2022; Sensors 2022)

Study	Power Meters	Gold Standard	Lab	Field	n	Power (W)	Cadence (rpm)	Data Averaging	Metrological Properties	Exercise Conditions
Abbiss et al. [59]	Velotron Ergometer (Racer-Mate, Inc., Seattle, WA, USA)	Calibration rig	x		15	250–1700	100–120	Max and full step	Accuracy Reproducibility	Sprint—Time trial 30 km
	SRM Scientific	Calibration rig	x		15	250–1700	100–120	Max and full step		Sprint—Power range—Time trial 30 km
Astorino and Cottrell [60]	Velotron Ergometer	Monark 894E (Monark, Vansbro, Sweden)	x		40	0–11 W·kg^{-1}	140–180	Average on Wingate (30 s) and peak value	Accuracy Reproducibility	Sprint (Wingate)
Attaway et al. [61]	Monark Ergometer and Velodyne Ergometer (Frontline Technology, Inc., Irvine, CA, USA)	Physiologic and perceptual responses	x		7	100–400	90 with Monark and Free with Velodyne	Full step	Accuracy Reproducibility	Power range
					6	125–225	90	Full step		Power range
Balmer et al. [62]	Kingcycle Air-Braked Cycle	SRM	x		9	400	-	60 s	Accuracy Reproducibility	-
Balmer et al. [63]	Kingcycle Air-Braked Cycle Ergometer	SRM	x		13	360–500	-	60 s	Accuracy	MAP-16.1 km TT
Balmer et al. [64]	Monark 814E	SRM Scientific	x		56	300–500	-	Average on Wingate (30 s) and peak values (1 and 5 s)	Accuracy	Sprint (Wingate)
Bernard et al. [65]	I-Crankset (SENSIX Society, Poitiers, France) and SRM	RTSL (Eaton Corporation, Troy Michigan, USA)	x		1	Unknown	56–90	Full step	Accuracy	Torque range—Cadence range
Bertucci et al. [36]	PowerTap PRO + (Saris Cycling Group, Madison, WI, USA)	SRM Scientific	x	x	1	100–420 + sprint	45–120	Full step	Accuracy Sensitivity Reproducibility	Power range—Sprint-Position (Seated vs. Standing)—cadence
Bertucci et al. [39]	Axiom Powertain (Elite, s.r.l., Fontaniva, Italy)	SRM Scientific	x		19	130–400	90 during MAP test ~90–100 during TT tests	Full step	Accuracy Reproducibility	Power range—Slope
Bertucci et al. [44]	New ergometer	SRM Scientific	x		1	100–300	90	Full step	Accuracy Reproducibility	Power range

Study	Power Meters	Gold Standard	Lab	Field	n	Power (W)	Cadence (rpm)	Data Averaging	Metrological Properties	Exercise Conditions
Czajkowski et al. [74]	PowerTap P1 (Saris Cycling Group, Madison, WI, USA)	SRM Professional	x		5	150–1250	60–100	Peak 1 and 5 s during sprints and full step during incremental	Accuracy Reproducibility	Participant—Power range—Cadence range-Sprint
Davison et al. [75]	Computrainer ergometer (Racermate Inc., Seattle, WA, USA)	SRM	x		1	200	~90	Full step (2 min)	Accuracy Robustness	Temperature—Calibration procedure
Dickinson and Wright [76]	Garmin vector 3	Lode Excalibur Sport			7	100–350 W + Sprints	Free	Full step (2 min) Peak power 10 s–on sprint	Accuracy Reliability	Large range of power on step of 2 min 10 s sprint all out
Drouet et al. [43]	Tacx Flow Ergotrainer (Tacx BV, The Netherlands) and Computrainer Pro	Calibration rig	x		-	100–600	80–130	Full Step	Accuracy	Power range—Cadence range
	SRM and PowerTap	Calibration rig	x		-	330–607	80–130	Full Step		Power range—Cadence range
Duc et al. [77]	Ergomo Pro (G-Sensortrchnik GmbH und Co. KG, Mörfelden-Walldorf, Germany)	SRM	x	x	1	100–900	47–123	Peak and mean 1 and 5 min	Accuracy Reproducibility	Power range—Sprint—Cadence range
Earnest et al. [78]	Lode Excalibur (Lode, Groningen, The Netherlands)	-	x		12	100–300	Free	Last minute of each step	Reproducibility	Power range
Finn et al. [79]	Repco air-braked ergometer (Repco Ltd., Huntingdale, Victoria, Australia)	Calibration rig	x		-	150–1500	70–150	Full step	Accuracy Reproducibility (two ergometers and two trials) Sensitivity	Barometric pressure-Cadence range—Power range
Fiolo et al. [80]	Tire pressure sensor (Arofly X-Elite New Taipei City, Taiwan)	SRM	x		12	50–300	50–100	60 s (eliminating first and last 15 s of the original sample of 90 s)	Accuracy Reproductibility Sensitivity	Steady state riding on trainer with various gearing and cadence
Franklin et al. [81]	Monark 824E	SRM Professional	x		8	~180	60	Last 3.5 min averaged	Accuracy Repeatability	-

Study	Power Meters	Gold Standard	Lab	Field	n	Power (W)	Cadence (rpm)	Data Averaging	Metrological Properties	Exercise Conditions
Hopker et al. [86]	Wattbike Cycle Ergometer (Wattbike Ltd., Nottingham, UK)	SRM Scientific	x		Calibration rig	50–1250	70–90 up to 700 W 90 above 700 W	Last minute of each step	Accuracy Reproducibility	Power range—Cadence range
	Wattbike Cycle Ergometer	SRM Scientific			20	50–340	70–105	Full step		Participant-Power range—Cadence range
Hurst and Atkins [87]	Polar S710	SRM Amateur	x		12	~550	~115	Max and full step	Accuracy	Power range
Hurst et al. [88]	Stages one-sided	SRM Professional		x	1	~230–450	~75–102	Max and full step	Accuracy Reproducibility (15 trials)	Peak and mean power of one off-road climb
Randolph et al. [89]	Garmin Vector	SRM Scientific	x	x	1	100–1150	47–123	Max and full step	Accuracy Reproducibility (10 trials)	Power range—Cadence range—Torque range—Field—Position—Sprint
Jones and Passfield [90]	SRM (2 Scientific and 1 Professional)	Monark 824E ergometer	x		-	90–630	90	Last minute of each step	Accuracy Repeatability (two trials)	Power range
Kirkland et al. [91]	Ergomo pro	SRM + Monark 814E	x		9	50–450	Free (~80)	Full step	Accuracy Repeatability (three trials)	Patten range—Power range—Balance L/R quantified with Lode
Lawton et al. [92]	SRM	Calibration rig	x		19 SRM1 Cal rig	50–900	100	Unknown	Accuracy Reproducibility	Power range
Lanferdini et al. [93]	Garmin Vertor	Lode Excalibur Sport	x		14	100–400	95 ±5	60 s	Accuracy reliability	Rampe test steady cadence Power range
Lillo-Bevia and Pallares [94]	Hammer Cycle Ergometer (CycleOps, Madison, WI, USA)	SRM Scientific	x		11	100–500	70–100	Full step excepted first 10 s and last 5 s	Accuracy Reproducibility (three trainers)	Power range—Cadence range—Position
MacIntosh et al. [95]	Monark (834E and 868) ergometers	-	x		5	600–1200	Free	Peak and mean 30 s (Wingate)	Accuracy	Sprint (Wingate)
Maier et al. [96]	SRM (12) Powertap (10) Quarq (11) Stages (13) Verve (3) Power2max (2) Garmin Vector (1) Keo Power (1) RotorPower(1)	Mathematical model	x		32	Up to 360	Free	Full step	Accuracy Repeatability (three trials) Reproducibility between power meters	Power range

Study	Power Meters	Gold Standard	Lab	Field	n	Power (W)	Cadence (rpm)	Data Averaging	Metrological Properties	Exercise Conditions
McGowan and Watson [97]	Wahoo KICKR Garmin, Pioneer, Quarq, SRM, Stages	Calibration rig	x		20	50–1000	90–120	Middle 30 s of each step Peak power for each sprint	Accuracy	Power range—Cadence range—Sprint—Time
McGregor and Rivera [98]	Computrainer	-	x		14	350–600	Free	Mean every 5 s and over the entire test	Accuracy Reproducibility (two trials)	Sprint (Wingate)
	Powertap	-	x		14	350–600	Free	Mean every 5 s and over the entire test		Sprint (Wingate)
Maxwell et al. [99]	35 friction-braked (Monark) ergometers	Calibration rig	x		Calibration rig	50–400	60	Last minute of each step	Accuracy Robustness	Power range—Oldness (old vs. new)—hysteresis effect (up vs. down)
	Five research-grade air-braked (Repco) ergometers	Calibration rig	x		Calibration rig	50–1150	50–150	Last minute of each step		Participant—Cadence range—hysteresis effect (up vs. down)
	Five electromagnetically braked ergometers	Calibration rig	x		Calibration rig	50–400	40–60	Last minute of each step		Participant—Cadence range
Merkes et al. [100]	Velocomp PowerPod (Velocomp LLC, Jupiter, FL, USA)	Verve Cycle InfoCrank (Verve Cycling, Perth, Australia)		x	12 and 4	100–1500	Free	Full step	Accuracy	Power range—Sprint
Micklewright et al. [101]	Lode Excalibur	Monark 814E	x		15	400–950	Free	Peak, minimum, and mean 30 s (Wingate)	Accuracy	Sprint (Wingate)
Miller et al. [102]	Quarq (Quarq, Spearfish, SD, USA) and Stages one-sided	PowerTap	x		4	~220	60–90	Full step	Accuracy	Participant—Cadence range
	Quarq and Stages one-sided	PowerTap		x	8	100–350	50–80	Full step according to the three profiles (UP, DH, and Flat)		Participant—Power range—Field profile-Frequency distribution
Millet et al. [103]	Polar S710	SRM Professional		x	8	200–440	Free	Max 5-s value and full step	Accuracy Repeatability (four trials) Sensitivity	Participant—Power range—Position

Appendix 2: Systematic Machine Design Concepts (Engineering Design, 2007)

6.2.3 Identifying the Essential Problems from the Requirements List

The clarification of the task with the help of a requirements list will have helped to focus attention on the problems involved and will have greatly increased the particular level of information (see Chapter 5). Elaborating the requirements list may thus be said to have prepared the way for following steps.

Here the task is to *analyse the requirements list* with respect to the required function and essential constraints in order to confirm and refine the crux of the problem. Roth [6.11] advises that the functional relationships contained in the requirements list should be formulated explicitly and arranged in order of their importance.

That analysis, coupled to the following step-by-step abstraction, will reveal the general aspects and essential problems of the task, as follows:

Step 1. Eliminate personal preferences.

Step 2. Omit requirements that have no direct bearing on the function and the essential constraints.

Step 3. Transform quantitative into qualitative data and reduce them to essential statements.

Step 4. As far as it is purposeful, generalise the results of the previous step.

Step 5. Formulate the problem in solution-neutral terms.

6.5 Developing Concepts

6.5.1 Firming Up into Principle Solution Variants

The principles elaborated in Section 6.4 are usually not concrete enough to lead to the adoption of a definite concept. This is because the search for a solution is based on the function structure, and so it is aimed, first and foremost, at the fulfilment of a technical function. A concept must, however, also satisfy the conditions laid down in Section 2.1.7—at least in essence—for only then is it possible to evaluate it. Before concept variants can he evaluated they must be firmed up, and experience has shown that this almost invariably involves considerable effort.

The selection process may already have revealed gaps in information about very important properties, sometimes to such an extent that not even a rough and ready decision is possible, let alone a reliable evaluation. The most important properties of the proposed combination of principles must first be given a much more concrete *qualitative*, and often also a rough *quantitative*, definition.

Important characteristics of the working principle (such as performance and susceptibility to faults), of the embodiment (such as space requirements, weight and service life) and finally of important task-specific constraints must all be known, at least approximately. More detailed information need only be gathered for promising combinations. If necessary, a second or third selection process should follow the collection of further information.

The necessary data are essentially obtained with the help of such proven methods as:

- rough calculations based on simplified assumptions
- rough sketches or rough scale-drawings of possible layouts, forms, space requirements, compatibility, etc.
- preliminary experiments or model tests used to determine the main properties or to obtain approximate quantitative statements about the performance and scope for optimisation
- construction of models in order to aid analysis and visualisation (for example, kinematic models)
- analoguc modclling and systcms simulation, oftcn with thc hclp of computcrs; for example stability and loss analyses of hydraulic systems using electrical analogies
- further searches of patents and the literature with narrower objectives
- market research of proposed technologies, materials, bought-out parts, etc.

Main headings	Examples
Function	Characteristics of essential auxiliary function carriers that follow out of necessity from the chosen solution principle or concept variant
Working principles	Characteristics of the selected principle or principles with respect to simple and clear-cut functioning, adequate effect, few disturbing factors
Embodiment	Small number of components, low complexity, low space requirement, no special problems with layout or form design
Safety	Preferential treatment of direct safety techniques (inherently safe), no additional safety measures needed, industrial and enviromental safety guaranteed
Ergonomics	Satisfactory man-machine relationship, no strain or impairment of health, good aesthetics
Production	Few and established production methods, no expensive equipment, small number of simple components
Quality control	Few tests and checks needed, simple and reliable procedures
Assembly	Easy, convenient and quick, no special aids needed
Transport	Normal means of transport, no risks
Operation	Simple operation, long service life, low wear, easy and simple handing
Maintenance	Little and simple upkeep and cleaning, easy inspection, easy repair
Recycling	Easy recovery of parts, safe disposal
Costs	No special running or other associated costs, no scheduling risks

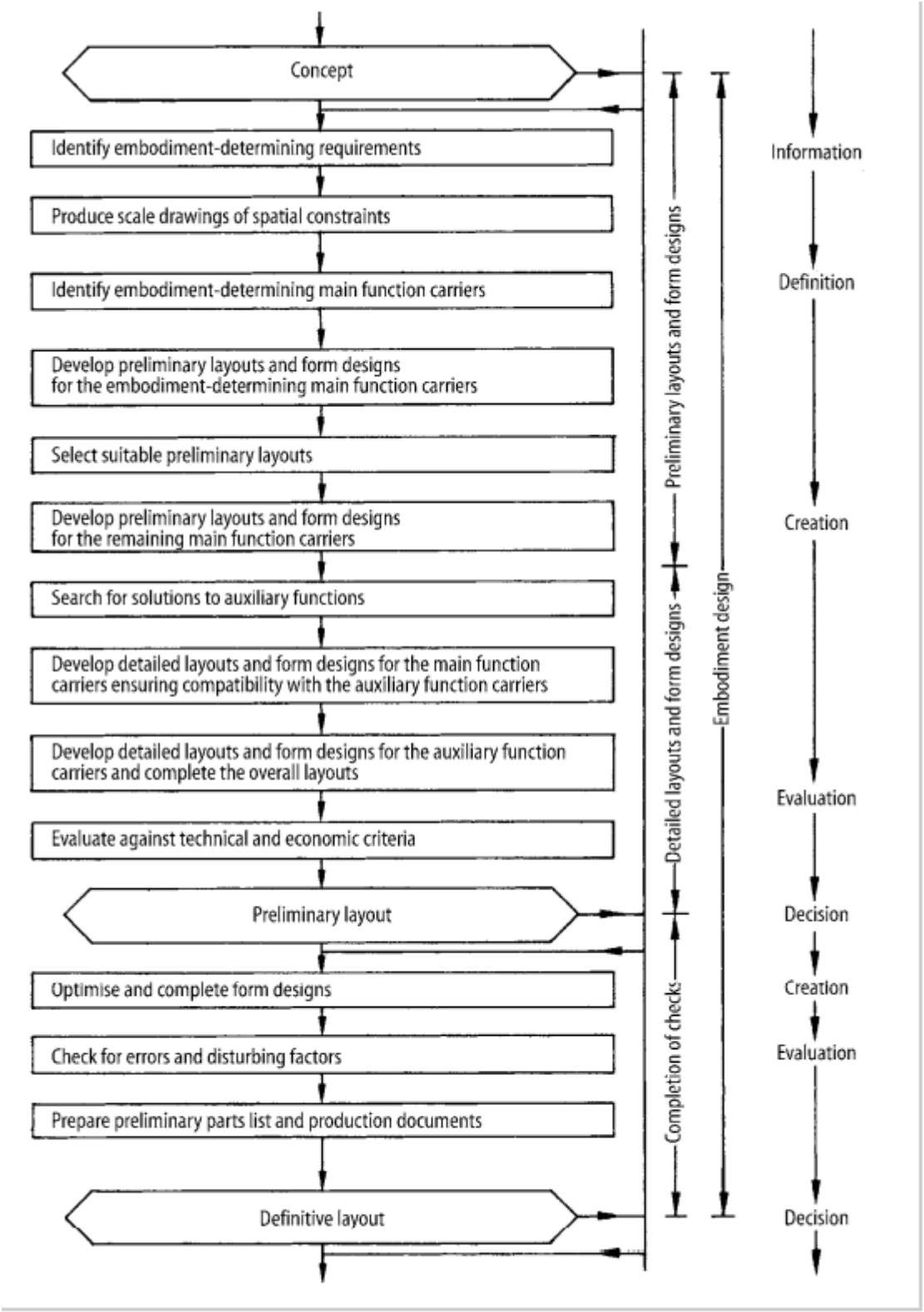

Figure 7.1. Steps of embodiment design

Embodiment design is the part of the design process in which, starting from the principle solution or concept of a technical product, the design is developed in accordance with technical and economic criteria and in the light of further information, to the point where subsequent detail design can lead directly to production (see Section 4.2).

The draft guideline VDI 2223: *Systematic Embodiment of Technical Products* [7.295] builds on recommendations from the fourth German edition of this book along with other sources. In doing so, it presents a generally established systematic procedure for embodiment design.

7.1 Steps of Embodiment Design

Having elaborated the principle solution during the conceptual phase, the underlying ideas can now be firmed up. During the embodiment phase at the latest, designers must determine the overall layout design (general arrangement and spatial compatibility), the preliminary form designs (component shapes and materials) and the production processes, and provide solutions for any auxiliary functions. During all of this, technological and economic considerations are of paramount importance. The design is developed with the help of scale drawings, critically reviewed, and subjected to a technical and economic evaluation.

In many cases several embodiment designs are needed before a definitive design appropriate to the desired solution can emerge.

In other words, the *definitive layout* must be developed to the point where a clear check of function, durability, production, assembly, operation and costs can be carried out. Only when this has been done is it possible to prepare the final production documents.

Unlike conceptual design, embodiment design involves a large number of corrective steps in which analysis and synthesis constantly alternate and complement each other. This explains why the familiar methods underlying the search for solutions and evaluation must be complemented with methods facilitating the identification of errors (design faults) and optimisation. The collection of information on materials, production processes, repeat parts and standards involves considerable effort.

The embodiment process is complex in that:

- many actions must be performed simultaneously
- several steps must be repeated at a higher level of information
- additions and alterations in one area have repercussions on the existing design in other areas.

Because of this, it is not always possible to draw up a strict plan for the embodiment design phase. However, it is possible to suggest a general approach with main working steps, see Figure 7.1. Particular problems may demand deviations and subsidiary steps, which can rarely be predicted precisely. The approach has to be planned to match the problem at hand, realising that further modifications will have to be made. Basically, the process will proceed from the qualitative to the quantitative, from the abstract to the concrete, and from rough to detailed designs. It is important to make provision for checks and, if necessary, for corrections.

1. Starting with the principle solution, and using the requirements list, the first step is to identify those *requirements that have a crucial bearing* on the embodiment design:
   - size-determining requirements, such as output, throughput, size of connectors, etc.
   - arrangement-determining requirements, such as direction of flow, motion, position, etc.
   - material-determining requirements, such as resistance to corrosion, service life, specified materials, etc.

   Requirements such as those based on safety, ergonomics, production, assembly and recycling involve special embodiment considerations, which may affect the size, arrangement, and selection of materials (see Sections 7.2 to 7.5).
2. Next, the *spatial constraints* determining or restricting the embodiment design must be identified (for instance clearances, axle positions, installation requirements, etc.).
3. Once the embodiment-determining requirements and spatial constraints have been established, a rough layout, derived from the concept, is produced with the emphasis on the overall embodiment-determining *main function carriers*, that is, the assemblies and components fulfilling the main functions. The following subsidiary questions must be settled, with due regard paid to the principles of embodiment design (see Section 7.4):
   - Which main functions and function carriers determine the size, arrangement and component shapes of the overall layout (for instance, the blade profiles in turbomachines or the flow area of valves)?

4. Preliminary scale layouts and form designs for the embodiment-determining main function carriers must be developed; that is, the general arrangement, component shapes and materials must be determined provisionally. To that end, it is advisable to work systematically through the items under the heading "layout" in the checklist shown in Figure 7.3. The result must meet the overall spatial constraints and then be completed so that all of the relevant main functions are fulfilled (for instance by specifying the minimum diameters of drive shafts, provisional gear ratios, minimum wall thicknesses, etc.). Known solutions or existing components (repeat parts, standard parts, etc.) must be shown in simplified form. It may be useful to start working on selected areas only, combining these into preliminary layouts later.
5. One or more suitable *preliminary layouts* must be selected in accordance with the procedure described in Section 3.3.1 (modified if necessary) by considering the relevant items in the checklist shown in Figure 7.3.
6. Preliminary layouts and form designs must now be developed for the remaining main function carriers that have not yet been considered because known solutions exist for them or they are not embodiment-determining until this stage.
7. Next, determine which essential *auxiliary functions* (such as support, retention, sealing and cooling) are needed and, where possible, *exploit known solutions* (such as repeat parts, standard parts, catalogue solutions). If this proves impossible, *search for special solutions*, using the procedures already described in Section 3.2 and Chapter 6.
8. *Detailed layouts and form designs for the main function carriers* must now be developed in accordance with the embodiment design rules and guidelines (see Sections 7.3 to 7.5), paying due attention to standards, regulations, detailed calculations and experimental findings, and also to the problem of compatibility with those auxiliary functions that have been realised. If necessary, divide into assemblies or areas that can be elaborated individually.
9. Proceed to develop the *detailed layouts and form designs for the auxiliary function carriers*, adding standard and bought-out parts. If necessary, refine the design of the main function carriers and combine all function carriers into overall layouts.
10. *Evaluate* the layouts against technical and economic criteria (see Section 3.2.2). If a particular project requires several concepts to be put in more concrete form prior to evaluation, then the embodiment process must not, of course, be pursued beyond what the evaluation of the variants demands. Depending on the circumstances, it is thus possible, in some cases, to take a decision just as soon as the main function carriers have reached the preliminary layout stage, while in other cases the decision will have to be deferred until after a great deal of detail design. In either event, all of the designs to be compared must be at the same level of embodiment, since no reliable evaluation is possible otherwise.

11. Fix the preliminary overall layout. The overall layout describes the complete construction structure (see Figure 2.13) of the system or product being designed.
12. Optimise and complete the form designs for the selected layout by *eliminating the weak spots* that have been identified during the course of the evaluation. If it should prove advantageous, repeat the previous steps and adopt suitable subsolutions from less favoured variants.
13. *Check* this layout design for *errors* (design faults) in function, spatial compatibility, etc. (see Figure 7.3), and for the effects of *disturbing factors*. Make what improvements may be needed. The achievement of the objectives with respect to cost (see Chapter 11) and quality (see Chapter 10) must be established at this point at the latest.
14. Conclude the embodiment design phase by preparing a preliminary *parts list* as well as a preliminary *production and assembly documents*.
15. Fix the *definitive layout* and pass on to the detail design phase.

Headings	Examples
Function	Is the stipulated function fulfilled? What auxiliary functions are needed?
Working principle	Do the chosen working principles produce the desired effects and advantages? What disturbing factors may be expected?
Layout	Do the chosen overall layout, component shapes, materials and dimensions provide: adequate durability (strength) permissible deformation (stiffness) adequate stability freedom from resonance unimpeded expansion acceptable corrosion and wear with the stipulated service life and loads?
Safety	Have all the factors affecting then safety of the components, of the function, of the operation and of the environment been taken into account?
Ergonomics	Have the human–machine relationships been taken into account? Have unnecessary human stress or injurious factors been avoided? Has attention been paid to aesthetics?
Production	Has there been a technological and economic analysis of the production processes?
Quality control	Can the necessary checks be applied during and after production or at any other required time, and have they been specified?
Assembly	Can all the internal and external assembly processes be performed simply and in the correct order?
Transportt	Have the internal and external transport conditions and risks been examined and taken into account?
Operation	Have all the factors influencing the operation, such as noise, vibration, handling, etc. been considered?
Maintenance	Can maintenance, inspection and overhaul be easily performed and checked?
Recycling	Can the product be reused or recycled?
Costs	Have the stipulated cost limits been observed? Will additional operational or subsidiary costs arise?
Schedules	Can the delivery dates be met? Are there design modifications that might improve the delivery situation?

Figure 7.3. Checklist for embodiment design

Appendix 3: Alternate 3-D Design and analysis of wheelchair-power meter assembly

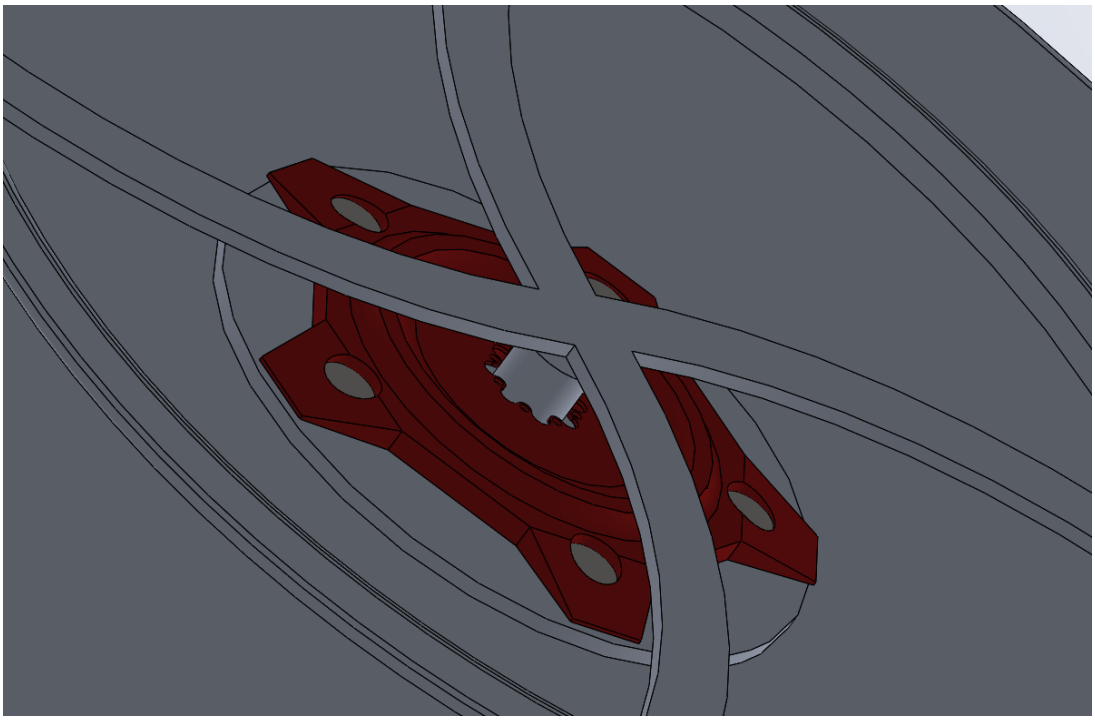

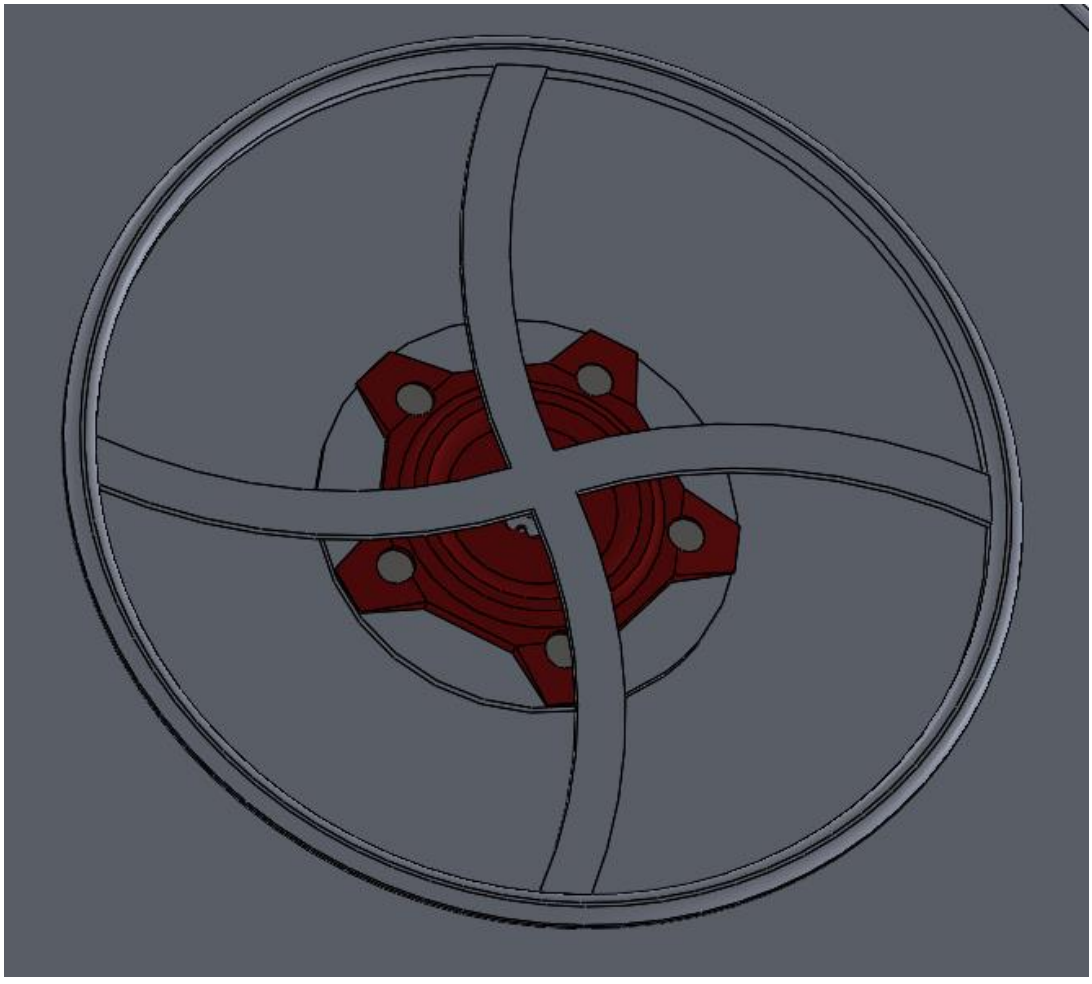

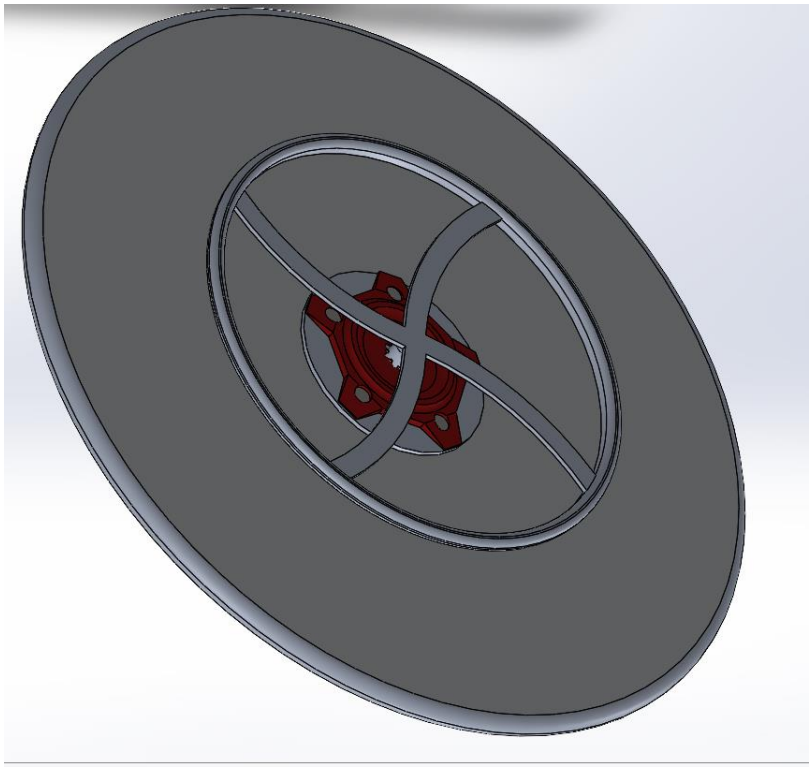

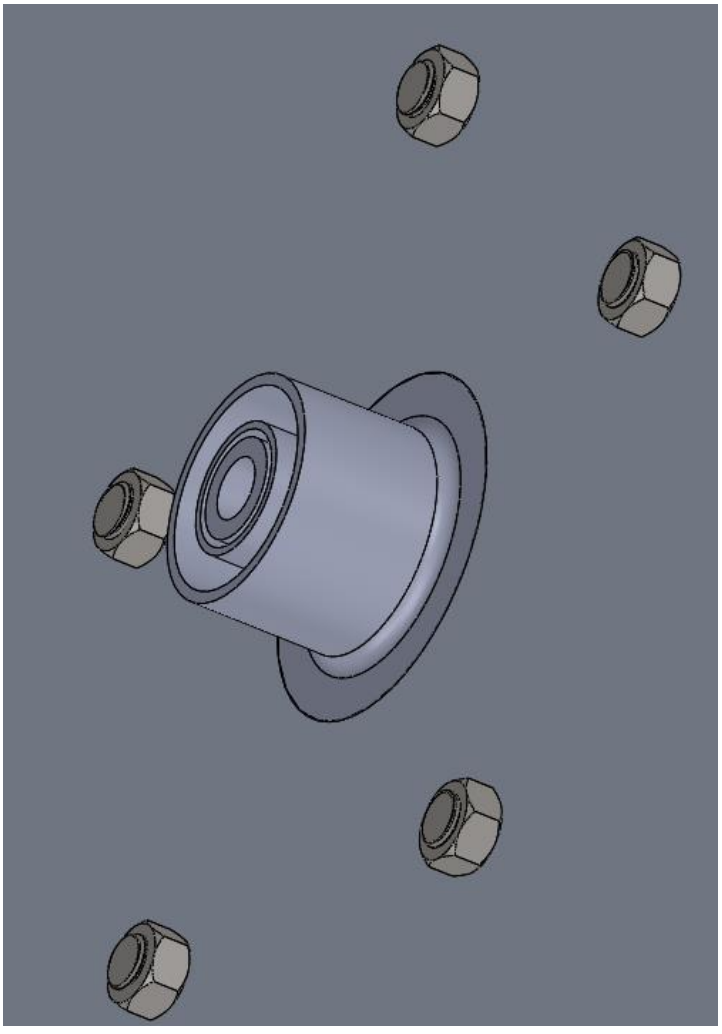

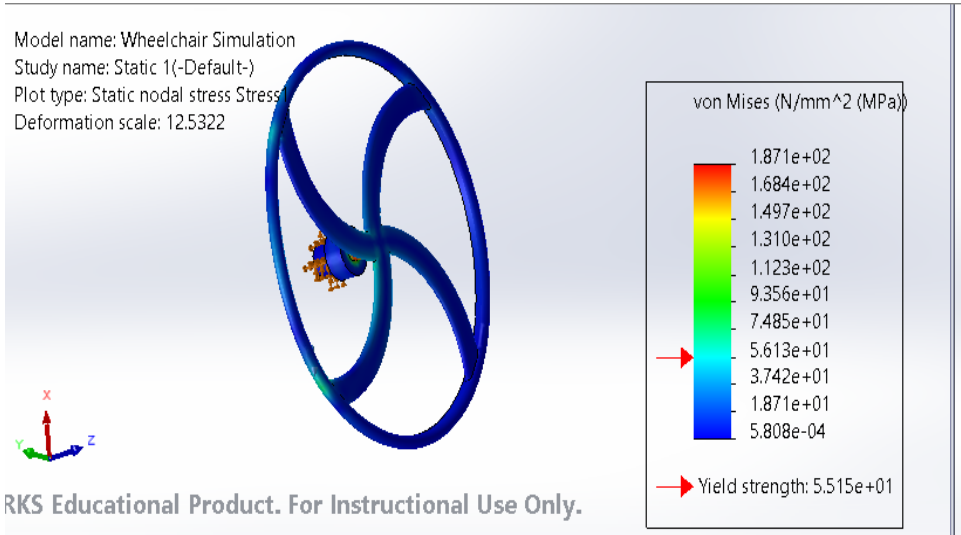
Model name: Wheelchair Simulation
Study name: Static 1(-Default-)
Plot type: Static nodal stress Stress1
Deformation scale: 12.5322
von Mises (N/mm^2 (MPa))
1.871e+02
1.684e+02
1.497e+02
1.310e+02
1.123e+02
9.356e+01
7.485e+01
5.613e+01
3.742e+01
1.871e+01
5.808e-04
Yield strength: 5.515e+01
RKS Educational Product. For Instructional Use Only.

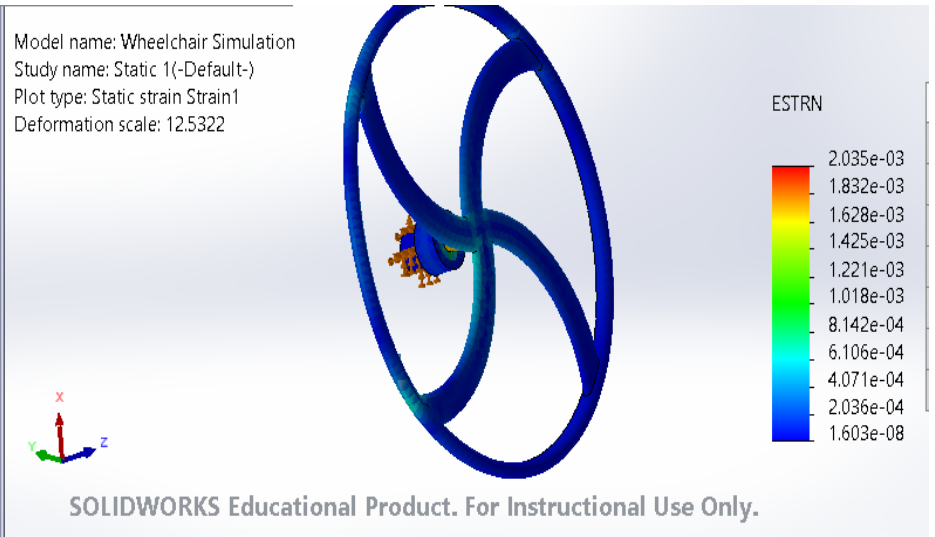
Model name: Wheelchair Simulation
Study name: Static 1(-Default-)
Plot type: Static strain Strain1
Deformation scale: 12.5322
ESTRN
2.035e-03
1.832e-03
1.628e-03
1.425e-03
1.221e-03
1.018e-03
8.142e-04
6.106e-04
4.071e-04
2.036e-04
1.603e-08
SOLIDWORKS Educational Product. For Instructional Use Only.

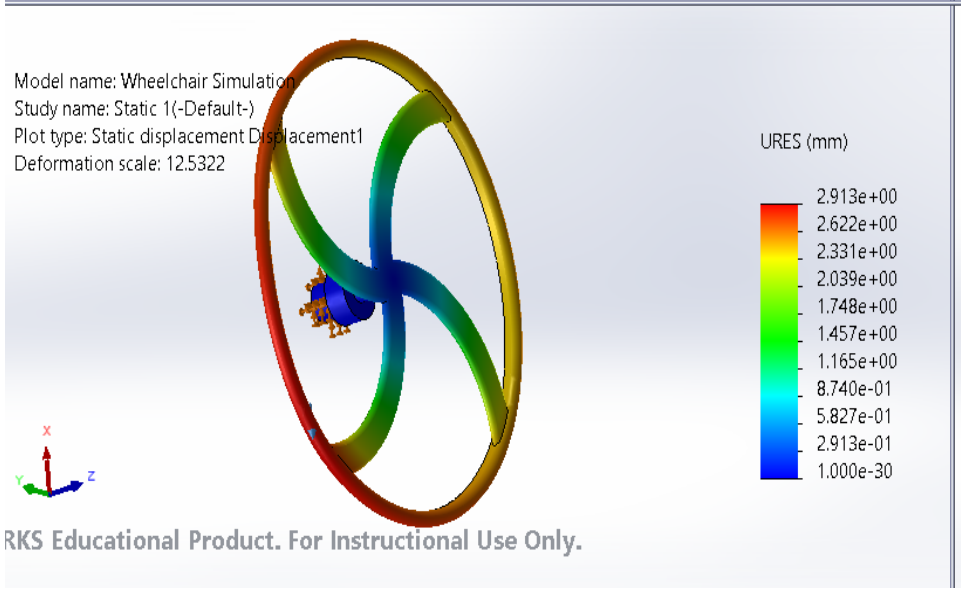
Model name: Wheelchair Simulation
Study name: Static 1(-Default-)
Plot type: Static displacement Displacement1
Deformation scale: 12.5322
URES (mm)
2.913e+00
2.622e+00
2.331e+00
2.039e+00
1.748e+00
1.457e+00
1.165e+00
8.740e-01
5.827e-01
2.913e-01
1.000e-30
RKS Educational Product. For Instructional Use Only.

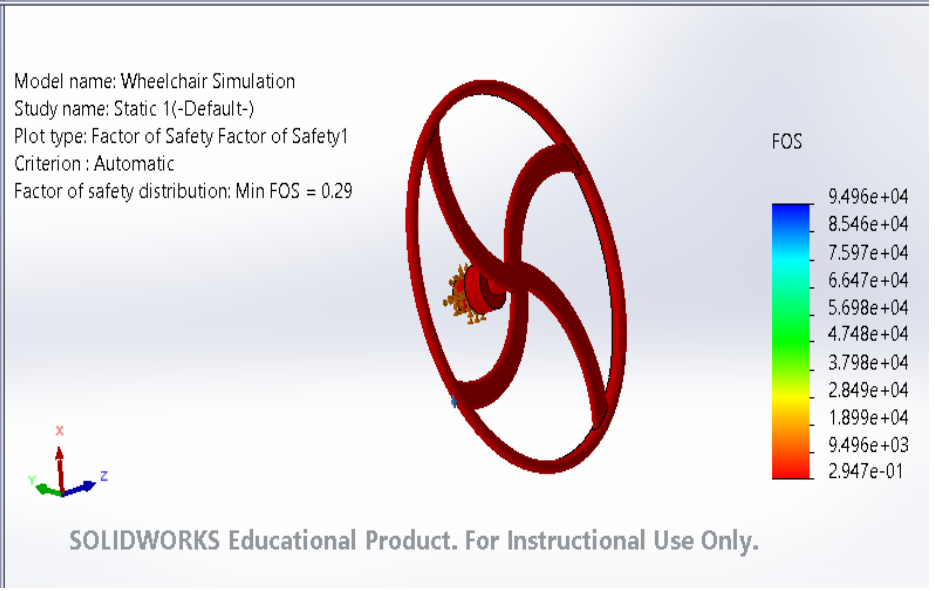
Model name: Wheelchair Simulation
Study name: Static 1(-Default-)
Plot type: Factor of Safety Factor of Safety1
Criterion : Automatic
Factor of safety distribution: Min FOS = 0.29
FOS
9.496e+04
8.546e+04
7.597e+04
6.647e+04
5.698e+04
4.748e+04
3.798e+04
2.849e+04
1.899e+04
9.496e+03
2.947e-01
SOLIDWORKS Educational Product. For Instructional Use Only.

Model name: Wheelchair Simulation
Study name: Topology Study 1(-Default-)
Plot type: Material Mass
Calculated Element Mass : 0.60371Kg

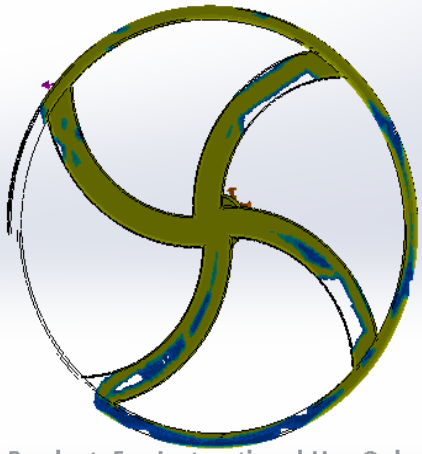

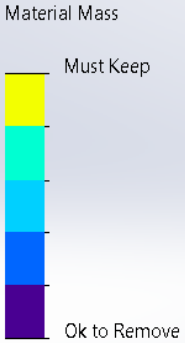

SOLIDWORKS Educational Product. For Instructional Use Only.

Model name: Wheelchair Simulation
Study name: Topology Study 1(-Default-)
Plot type: Material Mass
Calculated Element Mass : 0.80716Kg

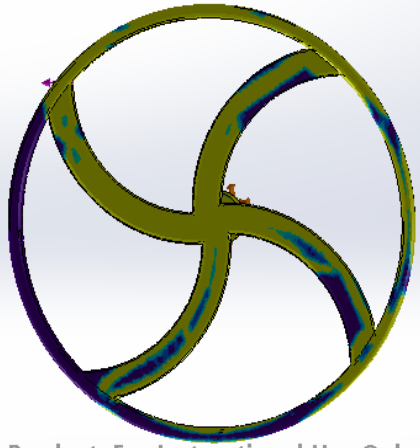

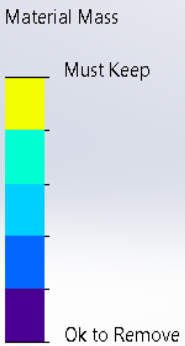

SOLIDWORKS Educational Product. For Instructional Use Only.